EVALUATION OF FLYWHEEL AND BATTERY SYSTEMS FOR POWER SMOOTHING OF A PHOTOVOLTAIC PLANT INTO POWER GRID

by

José R. Rivera Alamo

A project submitted in partial fulfillment
of the requirements for the degree of

MASTER OF ENGINEERING

in

ELECTRICAL ENGINEERING

University of Puerto Rico
Mayagüez Campus

2018

Approved by:

Fabio Andrade Rengifo, Ph.D. Chairman, Graduate Committee	Date
Eduardo I. Ortiz Rivera, Ph.D. Member, Graduate Committee	Date
Efrain O'Neill Carrillo, Ph.D. Member, Graduate Committee	Date
Maria A. Amador Dumois, Ph.D. Graduate Studies Representative	Date
Jose G. Colom Ustariz, Ph.D. Department Chairperson	Date

Abstract

The integration of renewable energy generation presents a great challenge in the energy management of an electrical system. The rapid variability in the production of energy from renewable resources, specifically solar, produces ramps that can cause instability in the electric system due to the inability of conventional generators to assimilate these rapid changes in a short period. As a result, the electric power company limits integration by renewable energy producers.

The purpose of this research work is to compare the capabilities of a flywheel and battery for voltage regulation in the face of disturbances produced by a photovoltaic plant in the power grid. A ramp control strategy and a static synchronous compensating control (STATCOM) were used to evaluate the performance of both energy storage systems (ESS). The results showed that the flywheel has better performance than the battery thanks to its rapid capacity to absorb and supply energy at the same rate. Another important result is that the ramp control used makes a considerable contribution to the regulation of voltage, requiring less reactive power and injecting more active power to the network while maintaining the stability of the voltage at the point of common connection.

Resumen

La integración de la generación de energía renovable presenta un gran reto en el manejo de energía de un sistema eléctrico. Las rápidas variabilidades en la producción de energía de los recursos renovables, específicamente solar, produce rampas que pueden causar inestabilidad en el sistema electico debido a la incapacidad de los generadores convencionales de asimilar estos rápidos cambios en un corto periodo. Como resultado, esto obliga a la compañía de energía eléctrica a limitar la integración por parte de los productores de energía renovable.

El propósito de este trabajo de investigación es comparar las capacidades de un volante giratorio (Flywheel) y batería para la regulación de voltaje ante los disturbios producidos por un parque fotovoltaico en la red eléctrica. Una estrategia de control de rampa y un control compensador sincrónico estático (STATCOM) fueron utilizado para evaluar el desempeño de ambos sistemas de almacenamiento de energía. Los resultados demostraron que el volante giratorio tiene mejor desempeño que la batería gracias a su rápida capacidad de absorber y suplir energía a la misma razón. Otro resultado importante es que el control de rampa utilizado hace una considerable contribución a la regulación de voltaje, requiriendo menos potencia reactiva e inyectando más potencia activa a la red manteniendo la estabilidad del voltaje en el punto de conexión en común.

To my wife.

Table of Contents

List of Tables

List of Figures

Chapter 1 - Introduction

In 2010, Puerto Rico adopted the Renewable Portfolio Standard (RPS) with the purpose of establishing a requirements percentage of renewable energy of the total demand of Puerto Rico Energy Power Authority (PREPA). As establish ACT #82, RPS requiring PREPA to get 12% of renewable energy integration starting in 2015, 15% by 2020 and 20% by 2035 [1]. At the present time, some private companies integrate solar and wind energy into Puerto Rico utility grids covering only around 2% of the total energy demand [2], which means that PREPA is not complying with the integration amounts of renewable energy as stipulates the RPS.

The main power generation plants of PREPA have been operating for more than 40 years. Their generators staying useful but incapable to allow massive quantities of renewable energy due to ramping limitation. The percentages of renewable energies required by REP to be integrated into PREPA power grid, represent a big challenge from many point of view. Leading of those challenges, is the variable and intermittent nature of renewable energies. To fulfill the ACT #82, a possible solution to integrate huge percentage of renewable generation to the grid can be integrate Energy Storage Systems (ESS) to permit power generators assimilate power flow without affecting power quality. Currently, ESS has many applications on the field of power systems. Nowadays, one of the most common of them is to increase the integration of renewable energies to the grid. SIEMENS has performed a study of the renewable energy integration to PREPA power grid based on 12% of renewable injection, concluding that it is necessary include ESS to manage the energy that could not be delivered to the load. The second option that they provide is integrate two combine cycle plants of 334 MW that can ramp quickly and are flexible with the capability of daily cycling [3].

1.1. Objective

When PV generation increases, it is not easy for conventional generators in the system to track the rapid variation in PV penetration. The main objective of this study is to compare the contribution of Flywheels and Batteries to increase the penetration level of photovoltaic (PV) power generation into the power grid by considering power smooth and voltage stability strategies at the point of common connection. To achieve the main goal, we aim to:

- Develop a simulation with dynamics models to evaluate the behavior of the proposed topology. The same scenario will be prepared for flywheel and batteries.
- Calculate the size of energy storage system based on ramp rate permitted percentage.
- Identify different scenarios for a PV facility, for example the negative effect of PV integration without energy storage and control strategies.
- Compare the behavior and response for voltage stability and power smooth control of flywheel and batteries.

1.2. Literature Review

There exist many studies related to energy storage systems to mitigate power fluctuation and instability problems caused by large scales integration of renewable sources into the power grid. This section intends to summary a brief literature to the components related to this investigation.

The intermittent nature of PV power generation, is a significant issue when large grid scale integration is considering. The changeability of cloudiness is the main factor of the problem, generating prominent level of power fluctuation in a brief period compromising the grid stability at the point of common connection. In reference [4], the author develop an investigation of the power output fluctuation of PV plants in different time series and plant sizes. The study reveals

that the larger PV system is, the lower the fluctuation are. For 1-minute sample time, they record up to 90% and 70% fluctuations from a 1 MW and a 9.5 MW PV plant respectively, whilst in 45.6 MW plant fluctuate up to 33% [5]. With this information, it would help to estimate the energy capacity of our energy storage system for PV power smooth application.

As increase the interest of PV to power generation, also increase the studies to mitigate the problem associated with power fluctuations. Reference [6] provide a brief review on smoothing output power fluctuation methods of PV source. Some of the methods are, geographical dispersion, energy storage technologies, diesel generator, fuel cell and curtailment active power. Curtailment method is not recommended since the owner revenue are limited. Also, diesel generator, fuel cell and natural gas engine are not able to deal with fast ramp up and down due to the time taken by these sources to respond. Energy storage device are more appropriate to mitigate the problem induced by PV generation into the power grid.

In reference [7] the author perform a control strategy for the flywheel system to absorb or inject real power, thereby mitigating voltage swings created by variable power supply from wind generator. The study results assure that flywheels can provide voltage regulation for voltage sags that can be caused by large scale wind turbine generator. As an additional contribution for our research in this area, we consider PV generator instead wind and compare the results between flywheels and battery to perform voltage control and ramp rate control.

In reference [8] present a smoothing method in where performance of ultracapacitor, battery and flywheel are studied for a single large PV plant. The results showed that ramping violations are more dependent on ESU power capacity, not energy capacity. On the cost analysis, the capital cost of the batteries is cheaper than flywheel installation. But the operation and maintained, life cycle, electricity market, ramp rate limits and how ESU its used can influence the economic analysis.

Chapter 2 - Theoretical Background

2.1. Puerto Rico Electric System

At the end fiscal year 2013, PREPA essentially supply all energy to around 1,485,150 consumers in Puerto Rico. Until the end of this fiscal year, PREPA generate approximately 66% of the electricity and purchase the remaining on wish almost 0.7% came from renewable energy. PREPA has many challenge of design, operates, and maintain its system due to Puerto Rico geography, climate, and the dispersion of its population which is highly concentrated in metropolitan area of San Juan with 58% inhabitants, followed by urban areas of Ponce and Mayaguez with 12% and 7% of the population, respectively.

More than 90% of the transmission and distribution system of PREPA, are above ground, which make them more vulnerable to high speed winds, torrential rains, and erosion that can be caused by hurricanes and tropical storms. The geographical position of Puerto Rico, place it on the path of many of those natural disaster which has a season from June through November. On September 2, 2017, Hurricane Maria was the last to affect the island's economy and the Puerto Rico Electric System.

Puerto Rico transmission system is an interconnected network of 230 kV, 115 kV, and 38 kV power lines that transport electricity form power plants to distribution centers and then to reach customers. The transmission systems its divide to approximate of 375 circuit miles of 230 kV lines, 727 circuit miles of 115 kV lines, and 1,376 circuit miles of 38 kV lines. Additionally, around 35 miles of underground 115 kV cable, 63 miles of underground 38 kV cable, and 55 kV miles of 38 kV submarine cable are included to the transmission system. Installed high voltage transformer at the transmission system and power plants have a total capacity of 19,207 MVA. Distribution

system is divide by approximately of 31,550 circuit miles of operating voltage range from 4.16 to 13.2 kV, more than 1,800 circuit miles of underground lines, and 333 substations with a total installed capacity of 5,018 MVA. Figure 1, illustrate PREPA's transmission system including its projections for the year 2018.

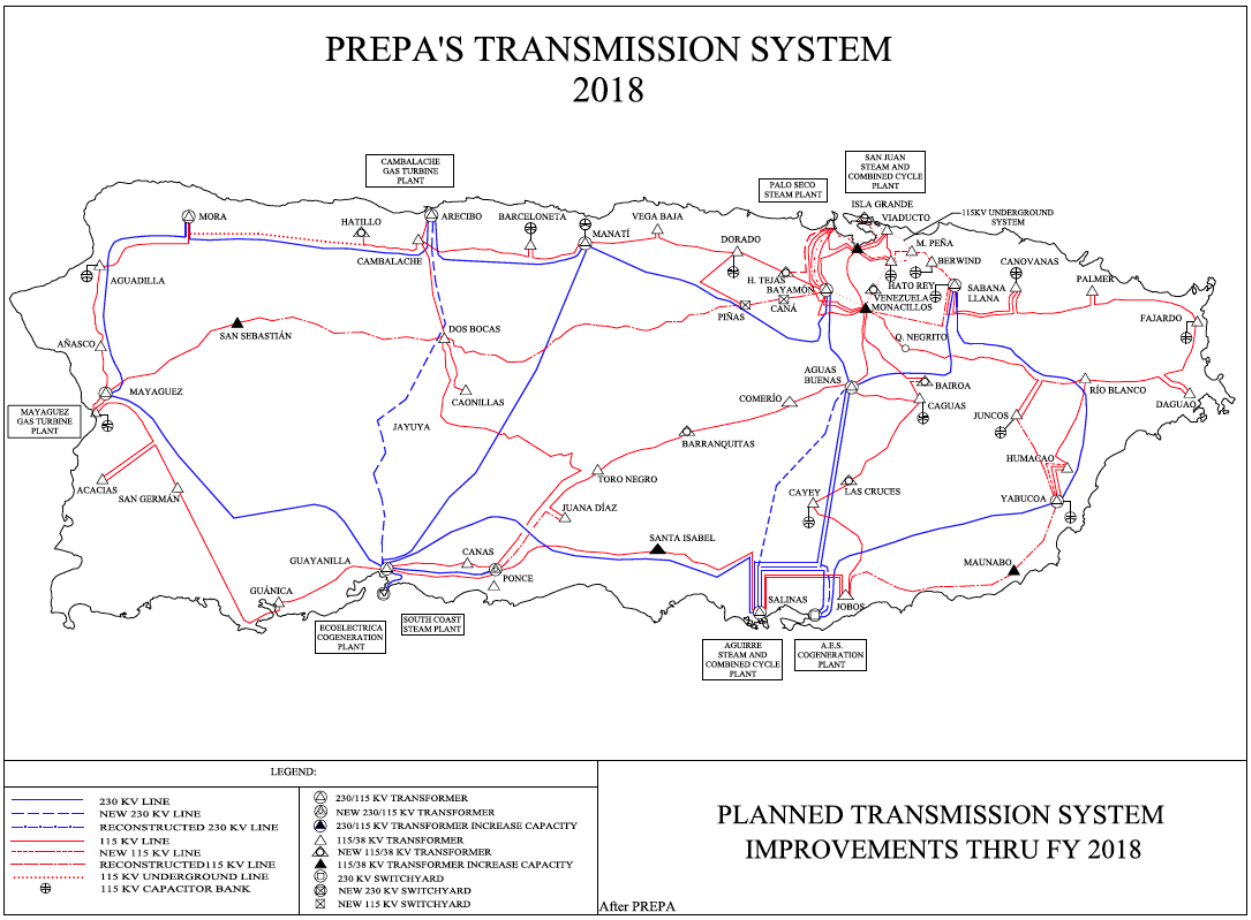

Figure 2-1: PREPA's Transmission System.[9]

PREPA's generation power plant's produce dependable capacity, proximate to 4,878 MW divided in 2,892 MW of steam-electric capacity, 846 MW of combustion-turbine capacity, 1,032 MW of combined-cycle capacity, 100 MW of hydroelectric capacity, and 8 MW of diesel capacity. Under the terms and conditions of Power Purchase Operating Agreements (PPOAs) PREPA supplement its own capacity. Appendix VIII in reference [9] has a description list of system

capability for each generation plant in which are included PREPA owners plant's and private plant's. Under PPOAs few projects of renewable energy provide a significant amount of power to the system. Renewable resource in operation are Pattern wind farm in Santa Isabel with nominal rating of 75 MW, Punta Lima wind farm in Naguabo with nominal rating of 26 MW, the 1MW wind turbine at the Bechara water treatment facility in San Juan, the AES Iluminia 20 MW solar farm in Guayama and the 2.1 MW Windmar solar farm near Ponce. All those projects are considered intermittent source of power because they are based on the availability of wind and sun resource, consequently they are considered unreliable capacity. PREPA a list of renewable energy contracts under power purchase agreements [10]. The list includes wind and solar farms in operation, also project scheduled for completion and operation in fiscal year 2015.

2.2. Minimum Technical Requirements for Distributed Generation

The following section summarizes the most relevant parameters of the minimum technical requirements related to this investigation for the integration of photovoltaic systems at any point of interconnection of PREPA. All of those requirements are taken from reference [11] and they are:

1. **Voltage Ride Through**

   PREPA's low voltage ride through requires all generation to remain online and operating on the following scenario:

   - Measured from point of interconnection (POI), three phases and single phase faults down to 0.0 per unit, for up to 600ms.
   - During and after normal cleared faults on the point of interconnection.
   - During backup cleared faults on the point of interconnection.

- During fault condition, operate on reactive current injection mode with droop characteristic which shall have an adjustable slop from 1 to 5% and a dead band of 15%.

For overvoltage ride through requires all generation to remain online and be able to ride through symmetrical and asymmetrical overvoltage condition specified by the following conditions:

- 1.4 – 1.3 pu 150 ms
- 1.3 – 1.25 pu 1 s
- 1.25 – 1.15 pu 3 s
- 1.15 or lower indefinitely

2. Voltage Regulation System (VRS)

Is required to have a constant voltage control. PV technologies in combination with Static Var Controls, such a Static Var Compensator (SVCs), Static Synchronous Compensator (STATCOMs) and Distribution STATCOM (D-STATCOMs) are acceptable options. VRS requirements includes:

- The system must have a continuously variable, continuously acting, close loop control VRS.
- At the POI, the VRS set point shall be adjustable between 95% to 105% of rated voltage. PREPA's Energy Control Center should be adjust the VRS set point via SCADA.
- The VRS operates only in a voltage set point control mode. Controller such power factor or constant VAR are not allowed.

- The strategy of VRS control shall be based on PI control action with parallel reactive droop compensation. The VRS droop shall be adjustable from 0 to 10%.
- At 0% droop, the VRS shall active a steady state voltage regulation accuracy of +/- 0.5% of the controller at the POI.
- The VRS shall be calibrate that a change in reactive power will achieve 95% of its final value no later than 1 second following a step change in voltage.
- The VRS must be in service at any time, the system is electrically connected to de grid regardless of MW output from the system.
- The VRS dead band shall not exceed 0.1%.

3. Reactive Power Capability and Minimum Power Factor Requirements

At the POI, the total range of power factor shall be from 0.85 lagging to 0.85 leading. The +/- 0.90 power factor range should be dynamic at the POI. In consequence the system must be capable to respond to power system voltage fluctuations by continuously varying the reactive output of the plant within the specified limits. It's required that the system reactive capability meets +/- 0.85 power factor range based in the system aggregated MW output, which the maximum MVAr capability is corresponding to the maximum MW output.

4. Short Circuit Ratio (SCR) Requirements

Short circuit ration under 5 can't be allowed. The installation of additional equipment, such as synchronous condensers, and controls necessary to comply with PREPA's minimum short circuit requirements must be assumed by the constructor.

5. Ramp Rate Control

The system must be able to control the rate of change of power output during some cases: 1) rate of increase of power, 2) rate of decrease of power, 3) rate of increase of power when a curtailment of power output is released, 4) rate of decrease in power when curtailment limits is engaged. The rate ramp control tolerance must be +10% and it limit apply independent if the meteorological conditions.

6. Power Quality Requirements

On the facility, the developer must address potential source and mitigation of power quality degradation prior to interconnection. Design must include applicable standards including, but not limited to IEEE standards 142, 519, 1100, 1159, and ANSI C84.1. Forms of power quality degradation include, but are not limited to voltage regulation, voltage unbalance, harmonic distortion, flicker, voltage interruptions and transient.

The previous technical requirements presented does not apply for every country in the world. Also, parameters vary with the interconnection voltage and power levels. In Mexico, some of the technical requirements at mid voltage level and power capacity between 30kW to 500kW are [12]:

- A steady state voltage under range of +/- 10%.
- Total range of power factor shall be from 0.95 lagging to 0.95 leading.
- A ram rate control adjustable from 1% to 5% per minute.

South Africa has some different requirements but, only specify if apply for distribution of transmission system [13]. Some of the requirements are:

- A steady state voltage under range of +/- 5%.

- Total range of power factor shall be from 0.95 lagging to 0.95 leading for a project between 100kW to 1MW.
- A ram rate control adjustable from 2% for every 30 seconds.

2.3. PV Power Generation

Nowadays, one of the most common and desirable renewable energy is the sun irradiance. The sun constantly radiates $3.83x10^{26}$ W in which earth receive $1.74x10^{17}$ W at the high atmosphere. Things like reflection, dust, cloudiness and pollution reduce power intensity that reach the earth surface approximately to $8.9x10^{16}$ W. Photovoltaics (PV) modules were created to transform sun's irradiance into electricity. A photovoltaic cell is essentially a photodiode which it simplest model is based on an ideal P-N junction diode. This model is best known as single diode PV model. To add complexity to the single diode model [14], a series and shunt resistance is added as shown in figure 2-2.

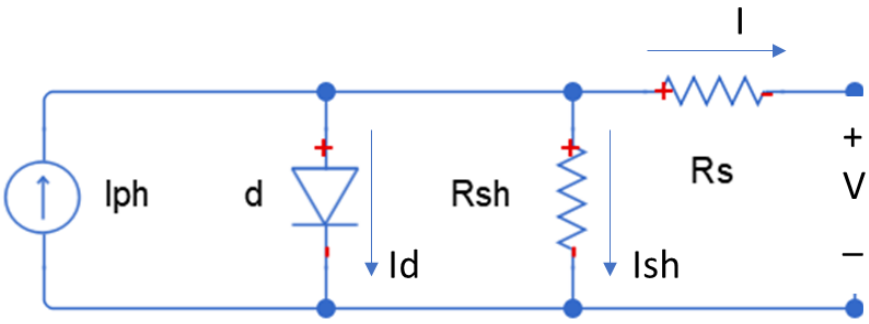

Figure 2-2: Single Diode PV Model.

From Kirchhoff's current law, a mathematical relationship of currents for this model is expressed by equation 2-1. In this equation, $\boldsymbol{I}$ is the PV module current, $\boldsymbol{I_{ph}}$ is the photocurrent produced by the solar irradiance, and $\boldsymbol{I_{sh}}$ is the shunt current flowing through the shunt resistor.

$$I = I_{ph} - I_d - I_{sh} \tag{2-1}$$

From this equation we can yield to equation 2-2 which describe the ideal behave of PV modules based on a current source in parallel with an ideal diode. In this equation, V_t is the thermal voltage of the P-N junction diode and ***m*** is the diode factor.

$$I = I_{ph} - I_d \left[exp \frac{V + I \cdot R_s}{mV_t} - 1 \right] - \frac{V + I \cdot R_s}{R_{sh}} \quad (2\text{-}2)$$

Each PV product has different electrical characteristics curve which describe it capacities relates to the current, voltage and power. A disadvantage of this model is that require iterative methods to generate I-V curves of one cell of specific module. There exists less complex analytical model that provide the dynamic behavior of PV module under different condition, including variations of solar irradiance and temperature. In reference [15], the author present some models of PV module that some of the parameters required can be obtained from the manufacturer data sheet and some others not. Also, the author proposes a model that only use the electrical characteristic provided by the PV module data sheet.

Each PV module build has its own current and voltage characteristic curves. The level of irradiation defines the max power that could produce a PV module and where will be located it optimal voltage and current value. Figure 2-3 presents I-V and P-V curves. As we can see, the maximum power produced at different irradiation level has different optimal voltage quantity. For this reason, is necessary to use a maximum power point technique to reach the maximum power that could be produced by a PV panel at different irradiation levels.

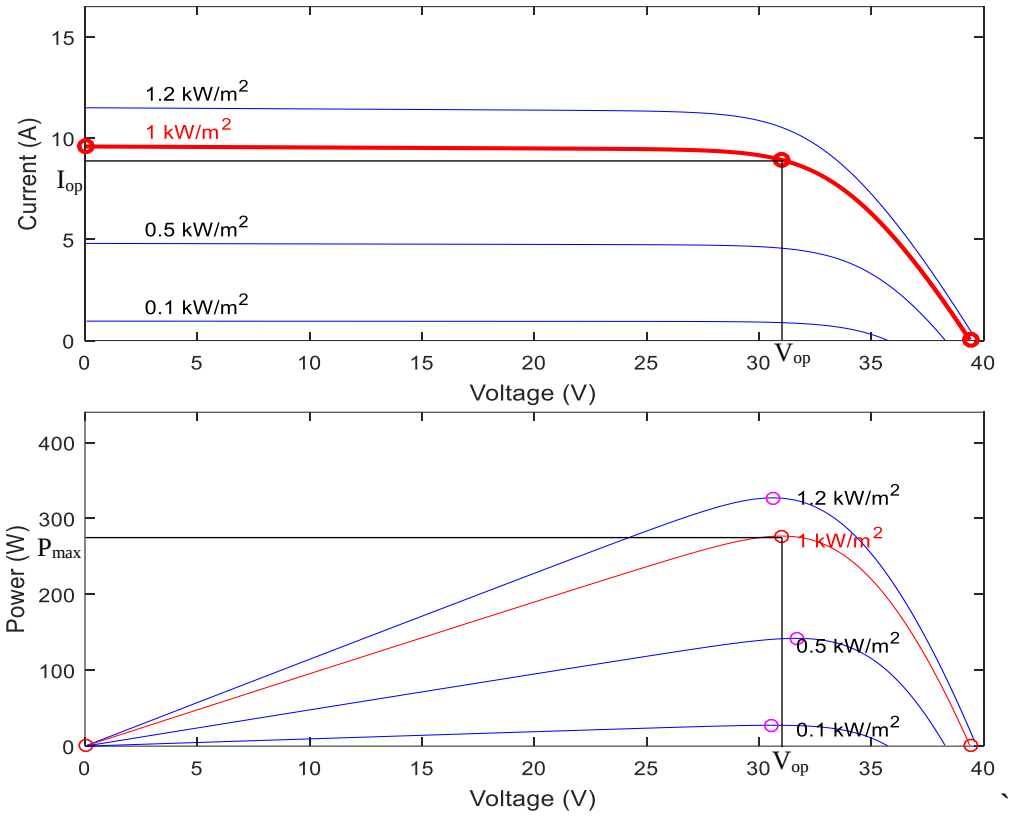

Figure 2-3: PV Characteristic Curves.

2.4. Energy Storage Systems

Most of the electric power produced in massive quantities are far from the consumption, making the transmission and distribution systems the weakest point in terms of energy losses in the form of heat. Small generation units, best known as distributed generation (DG) has become an alternative solution to this problem. Wind turbines and photovoltaic pharms are the most common DG among others. By its nature of intermittent generation, it is a challenge to maintain the power quality of the grid. Here it is where energy storage systems (ESS) play an important role in terms of power quality when great amount of renewable energies wants to be injected to the power grid. Many energy storage technologies have been developed for power systems applications. They are classified in short/long term usage as show Fig.2.4. Short-term Storage are used for applications where ESS are required to inject or absorb power in short time period, as in

power smoothing of wind turbines and PV systems. Moreover, Long-term Storage are usage for energy applications, such as load following and seasonal storage [16].

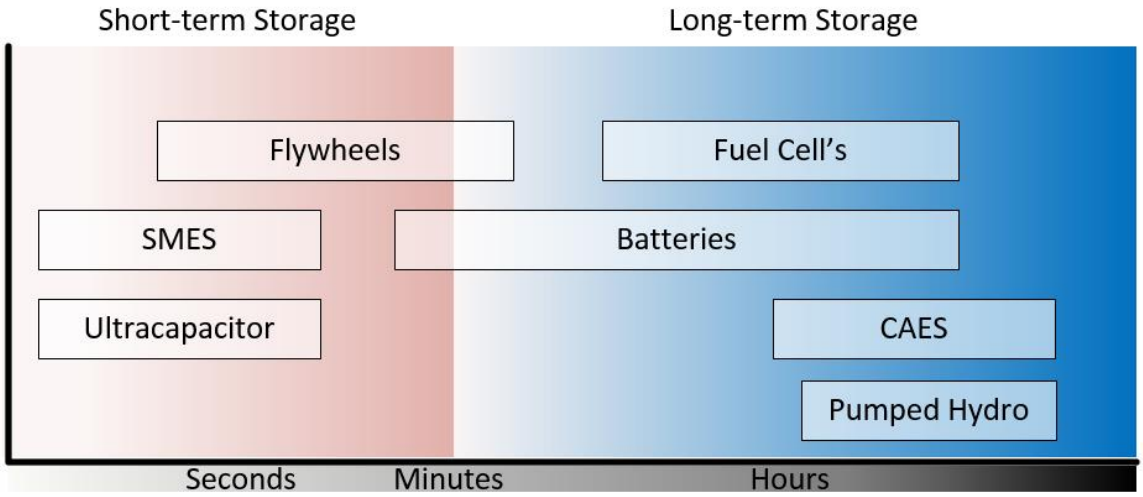

Figure 2-4: Classification of Energy Storages Technologies.

2.4.1 Flywheels

The flywheel energy storage system (FESS) is a rotating cylindrical mass at high speed which store energy in kinetic form. A flywheel is a heavy wheel typically placed in a vacuum chamber to reduce frictional loss. The amount of kinetic energy (**E**) stored in a flywheel varies linearly with the moment of inertia (**J**) and with the square of its angular velocity (**ω**); E, is given as:

$$E = \frac{1}{2} J \omega^2 \tag{2-3}$$

Flywheel mas and it geometry establish the moment of inertia. For a solid cylinder the moment of inertia has the following expression:

$$J = \frac{1}{2} r^2 m = \frac{1}{2} r^4 \pi a \rho \tag{2-4}$$

where ***m*** is the mass, ***r*** is the radius, ***a*** is the length and ***ρ*** is the density of the cylinder material. A speed limitation is given by stress developed within the wheel due to inertia loads known as tensile

strength. Therefore, a combination of a lighter materials with lower inertia load and speed up the flywheel is good for storing kinetic energy. A further information about flywheel governed equations and its technical considerations are presented in [17]. To store and release energy, a flywheel is couple to an electrical machine driven by two bidirectional power converters. When a flywheel work in charge mode, it's behave as a load and supply as source. Flywheels are classified as short-term energy storage device due to its capacity to exchange power continuously no more than a few minutes. A common flywheel topology is presented in figure: 2-5.

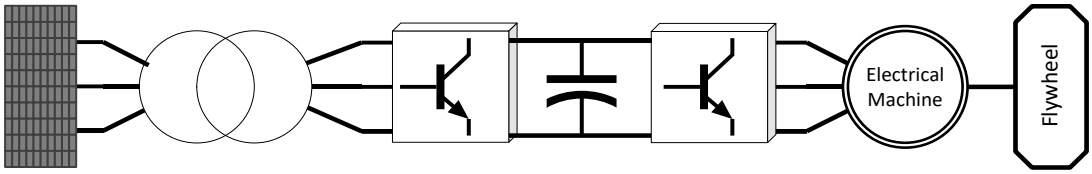

Figure 2-5: Flywheel Energy Storage System Topology.

Some advantage of flywheels are [17], [18]:

- Relatively low initial cost compared to the chemical storage system.
- The lifetime is almost independent of discharge cycle.
- High power and energy density.
- Easily measure state of chare, since it can be related with the rotational speed.
- Highly efficient (>85%).
- No require periodic maintenance.
- Charge/ discharge very quickly.

Some disadvantage of flywheel are [18]:

- Heavier compare to other energy storage systems.
- Present high stress and strains in high speed.
- It can't store large amount of energy.

2.4.2 Batteries

Battery energy storage system (BESS) stored energy in the form of electrochemical energy. Batteries are loaded with a cell arrange where electrical energy is transformed into chemical energy and vice versa. A connection of cells in series/parallel, define the battery voltage and current desired. Like flywheel system, when battery charge, behave as a load and as a source when supply energy. Some dynamic models of batteries have been developed, each one with different characteristic and approaches depending on the use of the model. In reference [19], the author present and cover further information of the most common electrical battery model. The simplest and commonly used model consists of an ideal resistor and voltage source connected in series as it is presented in figure: 2-4. This model does not consider the true internal resistance of the battery, which is strongly related with the state of charge (SOC). In reference [20], are discussed different battery technologies and present characteristic information such as its main components likewise its lifecycle based on the deep of discharge (DOD).

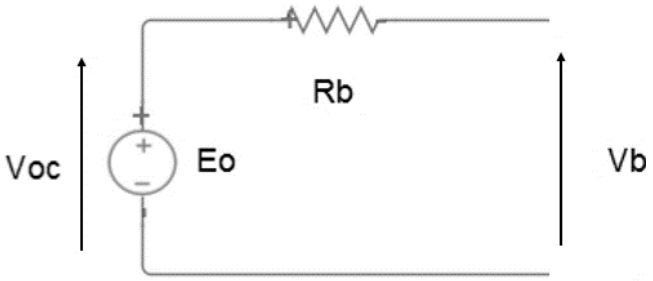

Figure 2-6: Simple battery model.

Each kind of battery has their own characteristic classified by capacity, type of base chemical or thermal response. Also, each kind of battery have their own characteristic discharge curve. This curve shows how varies the voltage of the battery over a constant discharge current as is presented in figure 2-6.

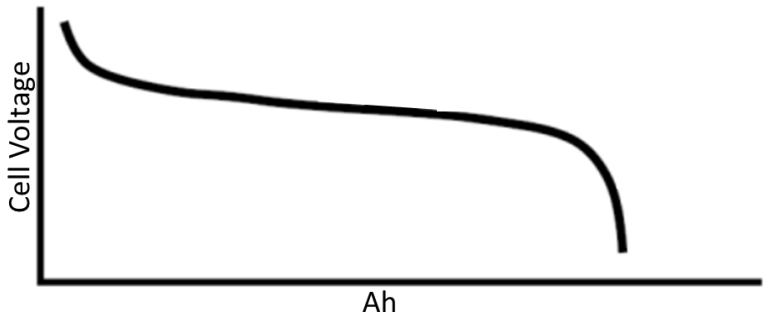

Figure 2-7: Current discharge curve.

Some advantage of batteries are [18]:

- High energy density.
- Relatively low self discharge rate.
- Can provide very high current for power applications.
- Highly efficient (>80%).

Some disadvantage of batteries are [18]:

- Require protection circuit to keep voltage and current within limits.
- Low life cycle
- Require cooling system to keep under safe operational levels.

2.5. Market of Energy Storage

Many studies have demonstrated the importance of energy storage for large scale renewable energy integration to the grid. The International Electrotechnical Commission (IEC) estimate the amount of energy storage in the world in 2050 to be around 189 GW or 305 GW, matching the output variations rate of renewable energies of 15% or 30% respectively [21]. Nowadays, the department of energy (DOE) have a global energy storage database which have registered 1652 projects for a total 193470 MW [22]. Energy storage systems addressed to aid the renewable energy generation are technologies on the marketplace that can be controlled from

network operators to enhance their capabilities, thus the grid assimilate the imbalance power between consumption and generation, also the effects related with it [23]. The capital cost of energy storage systems varies depending of what kind of technology is used to store energy. Furthermore, the present value of the system is strongly related to the end usages of the energy storage system. Usually, the bigger system is, higher is the revenue. Figure 2-7 shows us an idea of the size variation and it applications over the power grid interconnection level. Also, shows the type of income of operational benefit by different levels.

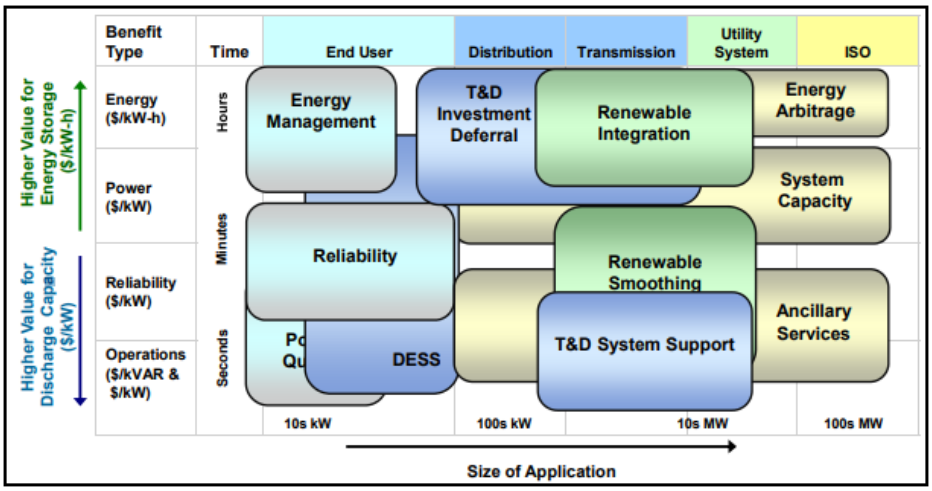

Figure 2-8: Operational benefits of energy storage [24].

Due to the variety of technologies to store energy and the coastally improvement of the strategies to implement over the diversity of application to use ESS, is hard to estimate the present cost of the energy to be used. A collaboration of the DOE, Electric Power Research Institute (EPRI) and National Rural Electric Cooperative Association (RECA) have developed the Electricity Storage Handbook to serve as a source guide for electric systems planners [25]. The handbook includes a variety of energy storage existing projects and a database of the cost of current storage systems of utility and customer services. Table 2-1 present a cost data for some of the energy storage technologies for transmission and distribution applications levels.

Table 2-1: ESS unit costs [25]**.**

Technology	Flywheel @ 100% DOD	Lead-acid @ 80% DOD	Li-ion @ 80% DOD
Total plant cost	$2,159/kW, $8,638/kWh	$5,023/kW, $502/kWh	$1,475/kW, $502/kWh
O&M	$5.8/kW-yr	$9.2/kW-yr	$8.3/kW-yr
Variable O&M	$0.0003kWh	$0.0005/kWh	$0.0110/kWh
Cycles / year	15,000	365	365

2.6. Power Quality

Power quality could be defined as those events which are reflected in voltage, current or frequency deviations out of acceptable levels. As increase the interest of integrate more and more renewable energy to the power grid, also increase the necessity of methods to mitigate the negative effects over the frequency and voltage. When power is added or absorbed from the power grid, the voltage and the frequency of the system will also fluctuate. Here is where energy storage, specifically those who has fast response take in place to keep the voltage and frequency of the system within limits. Due to the ability of the energy storage to respond to energy deficiency in the system, they are the preferred to deal with voltage problem although it may not be the cheaper solution [26]. Third party companies provide ancillary services to help keep power quality over power lines of the grid [27]. The Federal Energy Regulation Commission (FERC) define ancillary services as those "necessary to support the transmission of electric power from seller to purchaser given the obligation of control areas and transmission utilities within those control areas to maintain reliable operations of the interconnected transmission system" [28]. Due to the variety of energy storages and their specific qualities for each existing technology, is where they became more desirable for different power grid applications. Those energy storage most appropriate for power quality applications are flywheels, SMES, ultracapacitors and a variety of batteries [29].

Chapter 3 - Methodology

3.1. System Description

Due of the lack of short time period real data and information from PREPA, a small scenario is proposed to conduct our study. The used topology is presented in Figure 3-1. The system is composed of a main power plant which in this case represent PREPA. Also include a PV plant, an energy storage system (flywheel/Battery) with the corresponding control unit and variable load. All those components have a Point of Common Connection (PCC) through transformers. All models and scenarios are developed in MATLAB/Simulink.

Some of the assumptions of this topology are, a tree phase balanced connection, 38kV for primary winding of transformer at PCC, 480V for secondary winding of transformer and power plant generate at 38kV. The efficiency of ESS were not considered because the models were based on existing models. The following sections will explain the models used for each component of this system, also the corresponding sizing and other assumption.

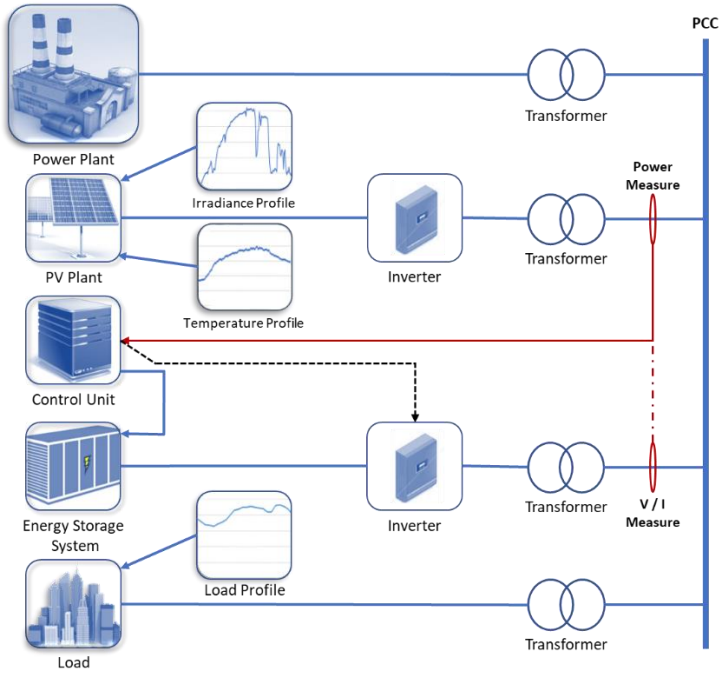

Figure 3-1: Proposed system topology.

3.2. Power Plant

Sometimes it's very rare to find a very specific information from PREPA like, specific models, real time data, or the transient response of the conventional generators to a power fluctuation. Without further information about PREPA generators, our power plant is model with a synchronous machine as the main power source driven by a diesel engine. The model was taken from an MATLAB/Simulink example and the control gains were tuned to give the generator a slower transient response. For our investigation, the synchronous machine is used to supply the power required from the load that PV generation can't cover. But, must important is to have the dynamics voltage variation produced by the limitation of the generator capacity.

3.3. PV Model.

The PV model used in this study is a dynamic model that can be performed by using the specifications provided by the PV model manufacturer's data sheet. Also, this model shows how the output power variates by changes in temperature and solar irradiance [30]. The PV output current in this model is described by equation (3-1). The variables I_x, V_x and V are the short circuit current, open circuit voltage and the output voltage respectively. The variables p and s are the number of PV modules connected in parallel and series. Finally, b is a constant characteristic related to specific PV module and is calculate by equation (3-2).

$$I(V) = \frac{p \cdot I_x}{1 - \exp\left(\frac{-1}{b}\right)}\left[1 - exp\left(\frac{V}{s \cdot b \cdot V_x} - \frac{1}{b}\right)\right] \tag{3-1}$$

All the variable in the following equation are constant values under standard test conditions (STC) that can be founded in the data sheet. The variable ε is the maximum error allowed where iterations will stop. An acceptable error is 0.01% and an initial value for b_n is 0.05.

$$while\ |b_{n+1} - b_n| > \varepsilon$$

$$b_{n+1} = \frac{V_{op} - V_{oc}}{V_{oc} \cdot ln\left[1 - \frac{I_{op}}{I_{sc}}\left(1 - exp\left(\frac{V_{op}}{b_n \cdot V_x} - \frac{1}{b_n}\right)\right)\right]} \tag{3-2}$$

The open circuit voltage V_x is expressed by the equation (3-3). In this equation, V_{max} and V_{min} are the open circuit voltage with an estimated value of $1.03 \cdot V_{oc}$ and $0.85 \cdot V_{oc}$ respectively. The variable *TCV* is the temperature coefficient of the open circuit voltage. T_N and E_{in} correspond to the temperature and effective irradiance under STC equal to 25°C and 1000 W/m^2. The only inputs variables of this model are T and E_i which are temperature and the effective solar irradiance.

$$V_x = \frac{E_i}{E_{in}} TCV(T - T_N) + V_{max} - (V_{max} - V_{min}) exp\left[\frac{E_i}{E_{in}} ln\left(\frac{V_{max} - V_{oc}}{V_{max} - V_{min}}\right)\right. \tag{3-3}$$

The short circuit current I_x is obtained from equation (3-4). The variable I_{sc} is the value of the short circuit current under STC and *TCI* is the temperature coefficient of the short circuit current.

$$I_x = \frac{E_i}{E_{in}} [I_{sc} - TCI(T - T_N)] \tag{3-4}$$

The output power of the PV model can be obtained by multiplying the PV output voltage by the current in equation (3-1). But, to obtain the maximum power from this model need to use the optimum voltage V_{op} as it is expressed in equation (3-5).

$$P_{max} = \frac{V_{op} \cdot I_x}{1 - \exp\left(\frac{-1}{b}\right)}\left[1 - exp\left(\frac{V_{op}}{b \cdot V_x} - \frac{1}{b}\right)\right] \tag{3-5}$$

The variable V_{op} is expressed in equation (3-6) where Re() is a function which extract the real part of complex number, and *lambertw*() is defined to be the solution *W(x)* of the nonlinear equation *W(x)exp(W(x))=x.*

$$V_{op} = Re\left(b \cdot V_x\left(lambertw\left(-0.3678944 \cdot exp\left(\frac{1}{b}\right) + 1\right)\right)\right) \quad (3\text{-}6)$$

To validate our model, a real model that can be founded on the market were selected. The specification of this model is presented in table 3-1.

Table 3-1: PV module specifications [31]**.**

SolarWorld	
Product Name	SW 275 Mono Black
Maximum Power	P_{max} = 275 W
Open Circuit Voltage	V_{oc} = 39.4 V
Maximum Power Point Voltage	Vmpp = 31.0 V
Short Circuit Current	I_{sc} = 9.58 A
Temperature Coefficient of V_{oc}	TCV_{oc} = -0.31 %/°C
Temperature Coefficient of I_{sc}	TCI_{sc} = 0.044 %/°C

With the previous specification, equation (3-1) were used to obtain the characteristic curves of this PV module. Figure 3-2 presents the resulting and its derivations from Ohm's law for power, voltage and internal resistance.

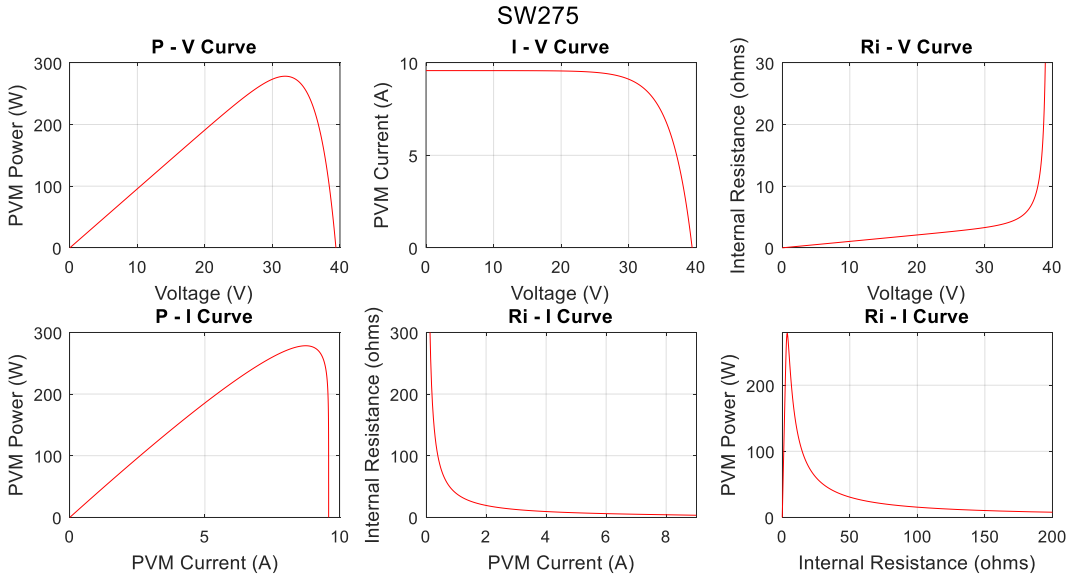

Figure 3-2: PV model characteristic curve validation.

Form equations (3-3), (3-4), (3-5) and (3-6) can be obtained the variations of open circuit voltage, short circuit current, max PV power and optimum voltage respectively from any combination of temperature and effective irradiation value. Figure 3-3 show the result of those equations.

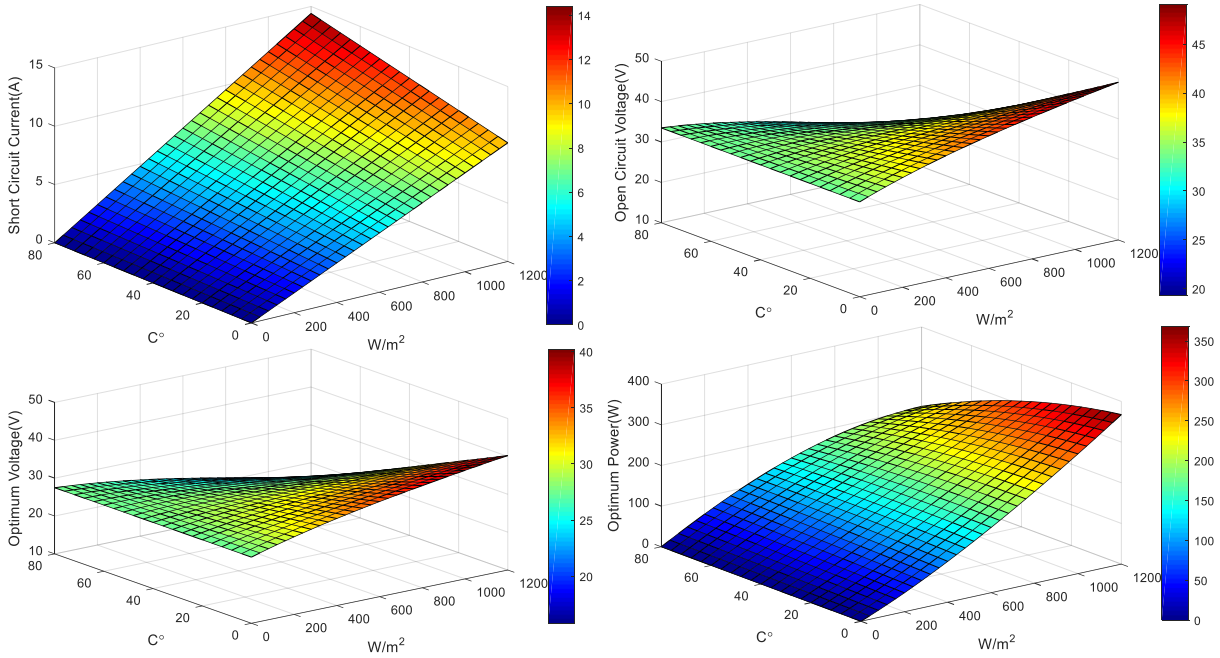

Figure 3-3: PV model behave under variations of temperature and irradiance.

3.4. Energy Storage System

3.4.1 Flywheel Model

Currently there is no flywheel model in MATLAB/Simulink. The Flywheel energy storage (FESS) model used in this study is based in equation (2-3), and then validated with the specifications in table 3-1 related with a Flywheel product of Beacon Power Corporation. There is no more specific technical information about the flywheel than the output voltage, max speed and energy/power ratings. A relevant feature of this flywheel, that is important to mention for this study is that the manufacturer assure the capability of charge and discharge at the same rate.

Table 3-2: Flywheel specifications [32]**.**

Beacon Series 400 Flywheel System	
Product Name	400 Modular
Grid Output/Supply Voltage	480 V_{ac}
Real Power Output /Discharge Time	160 kW for 5 min to 50 kW for 35 min
Usable Energy at Full Charge	30kWh
Spinning at Up to	16000 rpm

Taking parameters from table 3-1 in SI base units, the maximum energy storage **E=108 MJ**, and maximum rotational speed **ω=1675.5 rad/s**. Inertia value its estimated by rearranging the equation (2-3) in the form of equation (3-7). The estimated value of the inertia ***J=76.94 kg/m²***.

$$J = \frac{2E}{\omega^2} \tag{3-7}$$

The instantaneous power (P_{fw}), is the change in energy per unit time defined as:

$$P_{fw} = \frac{dE}{dt} \tag{3-8}$$

The torque produced by a rotating mass is given by:

$$T_{fw} = \frac{P}{\omega} = J\frac{d\omega}{dt} \tag{3-9}$$

Based on the previous equations, the flywheel model is simulated in MATLAB/Simulink as it is showed in figure 3-4 to validate the power ratings parameters summarized in table 3.2.

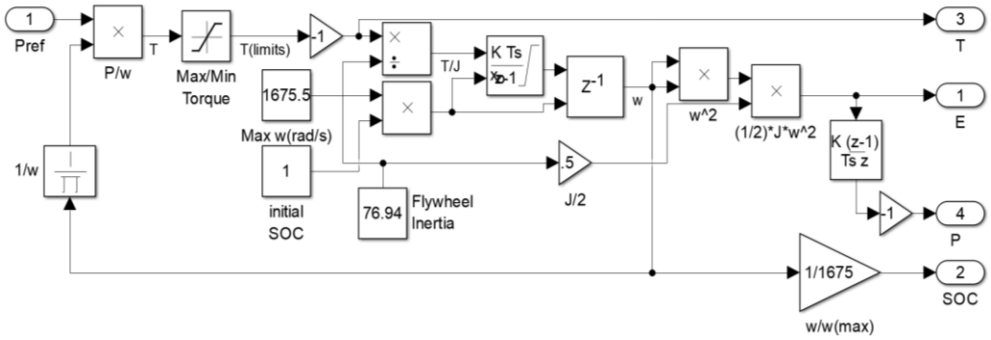

Figure 3-4: MATLAB/Simulink flywheel model.

To satisfy the power output/charge time provided by the manufacturer, a constant power reference of 160kW/50kW to verify the model. After few attempts, the reference torque was tuned and limited to ± 129 Nm to accomplish the constant power during the time of 5min/35min. The resulting outputs are presented in figure 3-5. The blue line represents the outputs of the flywheel with a reference power input of 160kW. The plot of power shows that the model can supply constant power through 300s (5 min) time lapse. The red line represents the output of the flywheel with a reference power input of 50kW. Also, in this case the model could comply with the time established to supply a constant power of 50kW during 2100 s (35min). Figure 3-5 also illustrate the behavior of energy, SoC and torque of the flywheel in the time frame for each reference power.

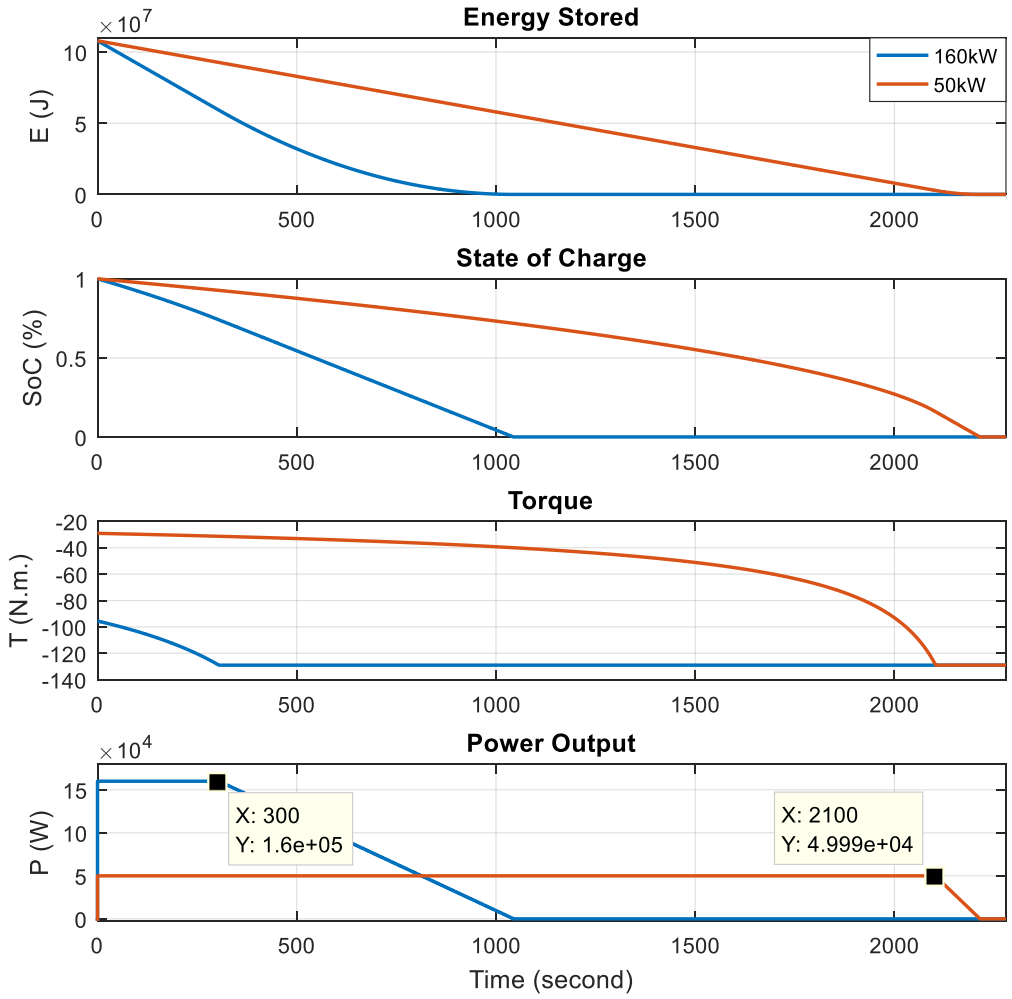

Figure 3-5: Flywheel model validation results.

3.4.2 Battery Model.

The used battery model is presented in reference [33]. This model was validated by the characterization of a 11 Ah Ni-Cd battery cell (SPH11) and for a stack of 210 cells. The stack model consists in a single cell model multiplied by N cells. The model is based on a Thevenin circuit with two parallel RC circuits connected in series. It includes a model for the hysteresis and an estimated SOC method counting ampere-hour. Figure 3-6, describe the proposed model by the author.

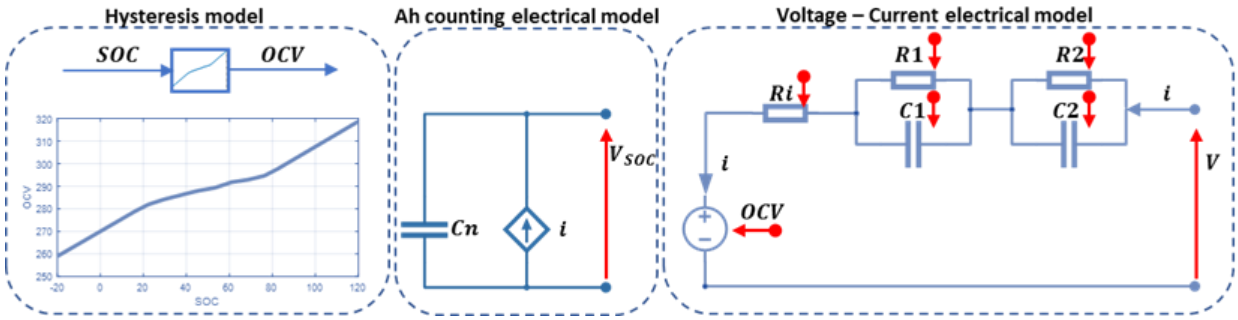

Figure 3-6: Model structure and equivalent circuit used in Simulink.

The hysteresis model consists of a function which receive a SOC value as an input and the output is a corresponding OCV to the SOC value. The function used is from real values taken by the characterization of the physical battery. The Ah counting model is related to the SOC of the battery and is described by equation (3-10). In this equation C_n is the nominal capacity of the battery, η is the efficiency and i is the current absorbed or supplied from the battery.

$$SOC_{t+\Delta t} = SOC_t \pm \frac{\eta}{C_n} \cdot \int_t^{t+\Delta t} i \cdot dt \cdot 100 \qquad (3\text{-}10)$$

From the Thevenin circuit in figure 3-6, can be obtained the output voltage of the battery model. Using the Kirchhoff's voltage law, the output voltage of the battery is expressed by equation (3-11). In this equation, V_{OCV} is the open circuit voltage related to the SOC, V_i is the voltage on

the internal resistance and V_1 *and* V_2 are the voltage for each RC parallel branch. Equation (3-12) describe the V_i, V_1 and V_2 voltages.

$$V = V_{OCV} - V_i - V_1 - V_2 \tag{3-11}$$

$$V_i = i \cdot Ri, \qquad V_1 = i \cdot R1\left(1 - e^{\frac{-t}{C1 \cdot R1}}\right), \qquad V_2 = i \cdot R2\left(1 - e^{\frac{-t}{C2 \cdot R2}}\right) \tag{3-12}$$

Table 3-2 summarize the specification of 1 cell battery taken from SPH11 datasheet. As it is mentioned previously, the battery model is based on a 210 cells array arranged in series. For our sizing calculation, one battery unit will be equal to a stack of 210 cells with estimated energy of usable stored energy of 2772 Wh (210*1.2V*11Ah).

Table 3-3: Battery specifications [34]**.**

SAFT Nickel-Cadmium SPH	
Product Name	Ni-Cd SPH 11
Capacity at the 5hr rate	11 Ah
Nominal Voltage	1.2 V_{dc}
Discharge Time @ final voltage: 1.0 V/cell	20.6 A for 30 min, 52.8 A for 5 min and 66.2A for 1 min

To test our battery model, a constant current was applied to the model to see it behavior. Figure 3-7 shows a few characteristics curves of this model. The first plot, displays the current discharge characteristics of our model with four different constant currents and the corresponding respond to each one. The second plot, shows the exponential zone which represents the hysteresis phenomenon for this Ni-Cd model in which the blue line represents the charging response, and the red one, represent the discharge. Last plot, shows us the direct relation between SoC and Ah with a constant current load in a time period.

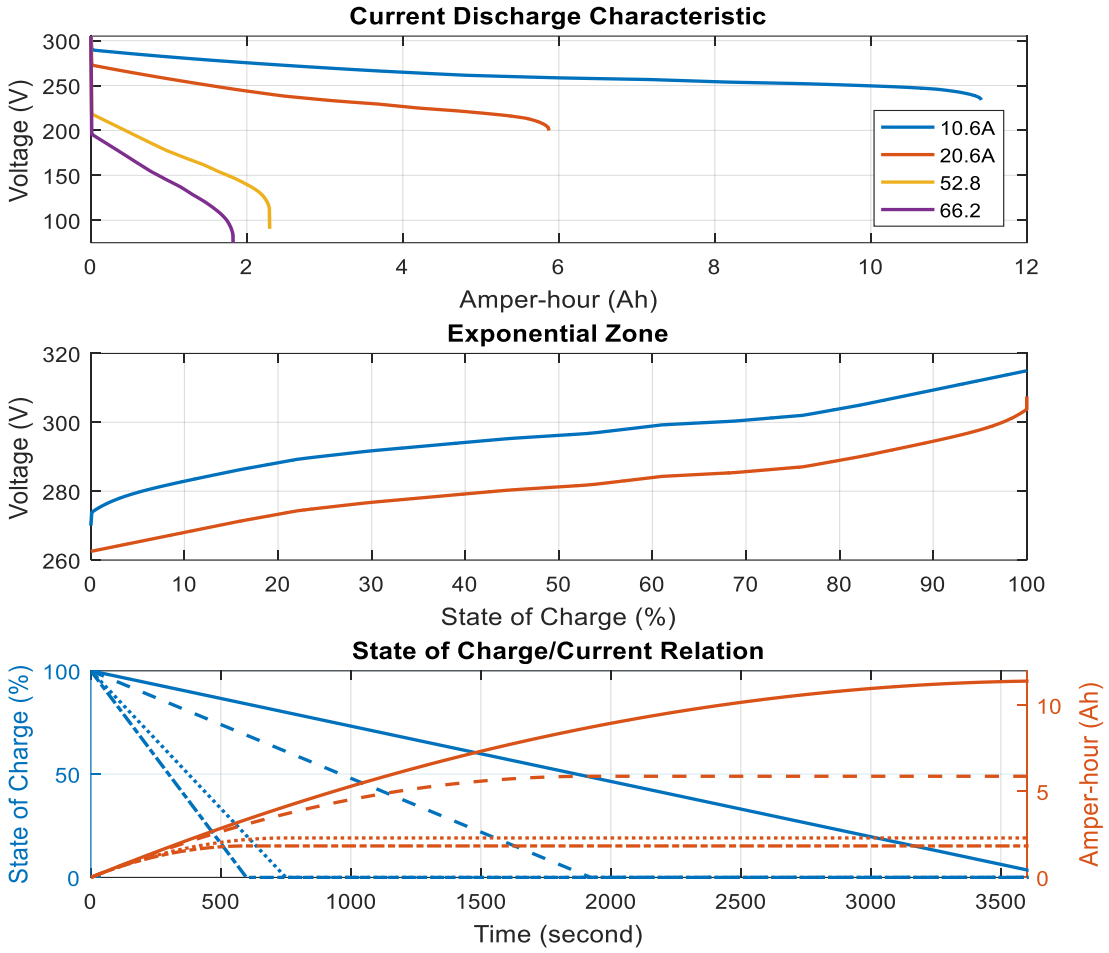

Figure 3-7: Battery model validation results.

3.4.3 ESS Topology and Control

The control used in this study for the power smoothed to be injected into the grid $P_G(t)$ is described by equation (3-13) and is known as moving average strategy. As the name indicates, it works by averaging a few samples from the input to produce outputs in a period ***T***. The function $P_{PV}(t)$ is defined by the variations of the generated power from the PV plant and the change in time T which is described by equation (3-14) were r_{max} is the maximum allowed ramp [35].

$$P_G(t) = \frac{1}{T}\int_{t-T}^{t} P_{PV}(t)dt \qquad (3\text{-}13)$$

$$T = \frac{5400}{r_{MAX}}\ (s) \tag{3-14}$$

A greater value of **T**, produce smother fluctuations at $P_G(t)$. To deal with voltage regulation at the PCC a traditional STATCOM strategy is used. Figure 3-8 shows the proposed configuration to manage the power absorbed/injected P_{ESS} into the ESS.

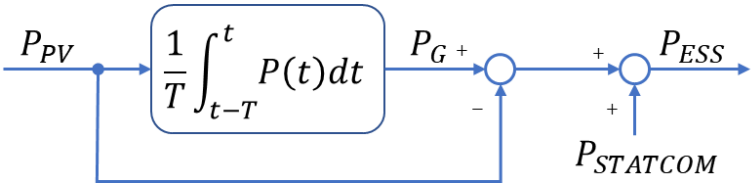

Figure 3-8: Power smooth/STATCOM control.

As presented the above image, P_{ESS} is the resulting sum of the power to be injected into the grid $P_G(t)$ by the smooth strategy and the equivalent real power required by the STATCOM technique. Equation (3-15) describe the reference power of the energy storage system. This proposed control, present an advantage to our simulation due to its relative easy implementation and effectiveness to its porpoise. But, in a full day simulation, this control needs to be limited by the hours of PV generation to avoid self discharge.

$$P_{ESS} = P_G - P_{PV} + P_{STATCOM} \tag{3-15}$$

The STATCOM control is used to regulate the voltage at the PCC by controlling the amount of reactive power injected/absorbed into the grid. Equation (3-16) define the real and reactive power of STATCOM control. Variable V_1 is the voltage at the PCC transformer side, V_2 is the voltage from the ESS side, X is the reactance of the transformer and σ is the phase angle of V_1 with respect to V_2. If V_2 is lower than V_1, STATCOM absorb reactive power. If V_2 is higher than V_1, STATCOM generate reactive power. Figure 3-7 illustrate the topology proposed to our ESS including used controls.

$$P = \frac{(V_1 V_2)\cdot \sin\sigma}{X}, \qquad Q = \frac{V_1 \cdot (V_1 - V_2 \cdot \cos\sigma)}{X} \tag{3-16}$$

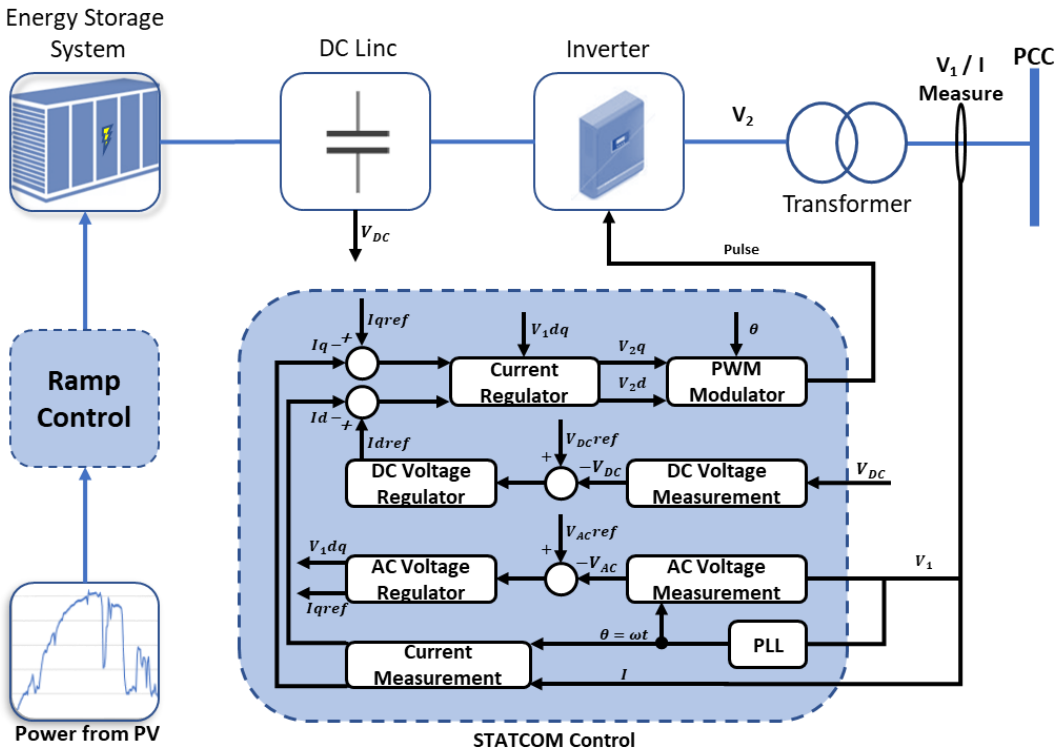

Figure 3-9: ESS control proposed topology.

3.5. Load Model

The load model used in this study is one with a given load profile that represent a residential load. The residential load follows a consumption profile with a given power factor of 95%. To maintain a constant power factor (pf) during all simulation, the input of our load model will be a real power (P) profile and the reactive power (Q) is calculated by the following equation:

$$Q = P \cdot \sqrt{\frac{1}{pf^2} - 1} \tag{3-17}$$

3.6. System Sizing

As it mentions before, this study intends to simulate a possible scenario of what could be a small part of Puerto Rico power grid with a PV integration. Following the topology proposed in figure 3-2, we will propose a size for the power plant of 100MW with 1 power generator. Based

on data from PREPA, on an average day, generator could reach 50% of its capacity or more. Our rated load will be 50MW and the rated PV array size will be 10MW which is 20% of the rated load as it is required from the energy portfolio for the coming years. To cover the amount of 10MW from the PV plant with the previous selected PV model it is required 38278 modules (10MW/261.252W).

Next step was to calculate the energy storage size required for our system. The method used is called the worst fluctuation model for PV plant. Starting with the worst fluctuation, described by equation 3-18 as a power exponential decay from P_{PV} to 0.1*P_{PV} (or decrease from 0.1*P_{PV} to P_{PV}) which means that the lowest point is remaining to diffuse irradiance by 10% of the produced power.

$$P_{PV}(t) = \frac{P^*}{100}\left[90\left(e^{-\frac{t}{\tau}}\right) + 10\right] \tag{3-18}$$

In this equation, P^* is the rated PV plant capacity (10MW) and τ (seconds) is directly related with the shortest side of the PV plant perimeter, l (meters), and have the following expression:

$$\tau = a * l + b \tag{3-19}$$

here a=0.042 s/m (inverse of estimated cloud travel speed) and b=-0.5 s (used to fit the correlation value of l) [36]. In our case we choose an l of 200 m (≈ sum of 200 PV modules, short side) which result a $\tau = 7.48\ s$.

The power demand required from ESS $P_{ESS}(t)$ correspond to difference between the maximum ramp-rate (10%/min) allowed by the power grid $P_G(t)$ and $P_{PV}(t)$. Therefore, $P_{ESS}(t)$ is describe by the following equation:

$$P_{ESS}(t) = \frac{P^*}{100}\left[90\left(1 - e^{-\frac{t}{\tau}}\right) - t * r_{MAX}\right] \tag{3-20}$$

where r_{MAX} is expressed in % per time. Thus, the maximum required power from ESS y expressed by:

$$P_{ESS,MAX}(t) = \frac{P^*}{100}\left[90 - \tau * r_{MAX}\left(1 + \ln\frac{90}{\tau * r_{MAX}}\right)\right] \quad (3\text{-}21)$$

Finally, the minimum energy to be stored in ESS is given by:

$$E_{ESS,min} = \int_0^{T_R} P_{ESS}(t)dt \approx \frac{0.9P^*}{3600}\left[\frac{90}{2 * r_{max}} - \tau\right] \quad (3\text{-}22)$$

Solving the previous equations, our ESS require a minimum energy storage capacity of 1,106,300 Wh (≈1.1MWh) and at least a capacity of power to be supplied of 8,566,896 W (≈8.6MW) to deal with the possible worst fluctuation that can take our PV plant. Figure 3-10 properly describe the equations above.

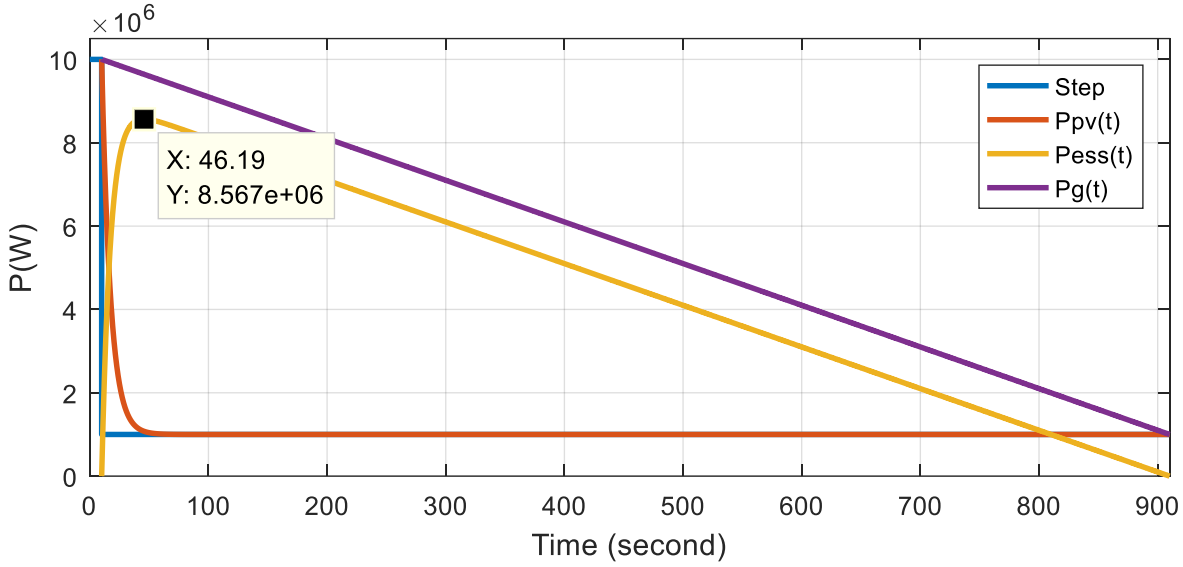

Figure 3-10: ESS sizing fitting curves results.

Knowing the capability for a single unit of our Flywheel/Battery, now we can proceed to quantify the size of our ESS based on each one specs and the requirements for the worst fluctuation of PV. First, to match the minimum energy requirements with flywheels it's necessary ≈37 units. But, the power that can cover that amount is below of the 8.6 MW required. For that reason, we

decide to match the minimum power which result in 54 units with 8.64 MW and 1.62MWh peak. For the battery, we try to match the same energy capacity with the flywheel and result in 1.622 MWh and an estimated peak power of 9.83 MW. Table 3-4 present a summary of each component of our system for the study.

Table 3-4: Summarize system sizes.

Component	**Capacity**		**Quantities**	**Total Capacity**	
Power Plant	100 MVA		1	100 MVA	
PV Module	275 W		36,364	10 MW	
Load	50 MVA		1	50 MVA	
ESS					
Component	**Power**	**Energy**	**Quantities**	**Total Capacity**	
Flywheel	160 kW	30 kWh	54	8.64 MW	1.620 MWh
Battery	16.8 kW	2.772 kWh	585	9.83 MW	1.622 MWh

Chapter 4 - Results

In this chapter, the results of the contribution of two different technologies of energy storage to help with the negative effect of PV integration will be presented and discussed. Some cases will be proposed to analyze the behavior of the voltage and P_G at the PCC to review the outcome of this study. The proposed cases are, a system (Gen/Load) with;

1. no PV plant and no ESS.
2. PV plant, no control and no ESS.
3. PV plant, only STATCOM control.
4. PV plant, ESS and only Ramp control.
5. PV plant, ESS and STATCOM/Ramp control.

4.1. Results

The fallowing sections, present and compare the proposed cases. Based on our focus to increase PV integration, all the simulations ran in a 13h (46,800s) time span which is the time of the sun rise (6AM) until the sunset (7PM) in Puerto Rico.

4.1.1 First Case

In this study, the first case will represent our base case scenario comprising just the generation and the proposed load profile. The load profile was shaped based on hourly data provided by PREPA and adjusted to have a rated power of 50MW. To have robustness in our results, a historic data was created with a few days overlapped which results in a 1-minute time series. Figure 4-1 shows the proposed load profile with the resulting voltage respond. As shows the voltage profile, at all moment, the voltage it's near to 1 p.u. which means the system is stable and the source can handle the variations of the load. The second scope present the respective active and reactive power of the load with the resulting 95% power factor.

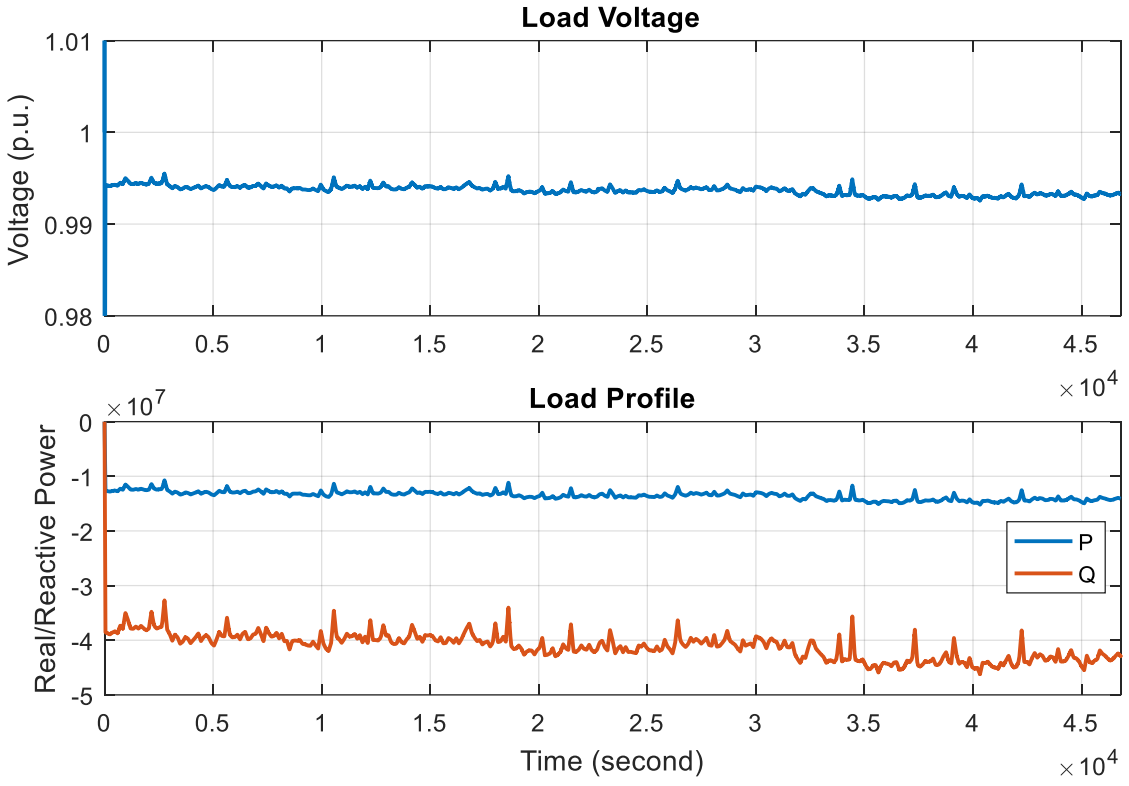

Figure 4-1: Load/ Voltage Profile Response.

Figure 4-2 shows the respective apparent power of the source/load. The different between the signal is because the simulation include step up/down transformers.

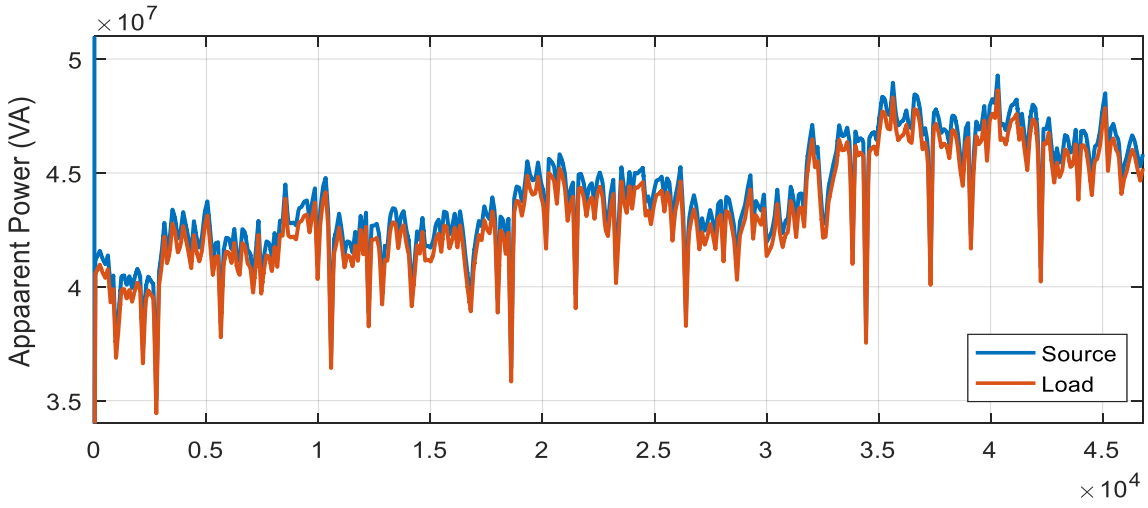

Figure 4-2: Source/ Load Apparent Power Profile Response.

4.1.2 Second Case

In this case, the idea is to present the PV generation profile and it possible negative voltage effect to a slow response conventional generator. The proposed power generation profile for our PV plant is presented in figure 4-3, it shows the resulting real power. The irradiance and temperature data used was a 5 minutes sample data collected from Mayaguez, Puerto Rico and intentionally added a drop percentage in power as partial shades. Three different percentages at different time was added as follow, 35% (3 min), 90% (5 min) and 45% (3 min) at hours 5 (18,000 s), 6 (21,660 s), 8 (28,800 s) respectively. A filter was added at the output to have an exponential ending as was calculated in equation 3-5.

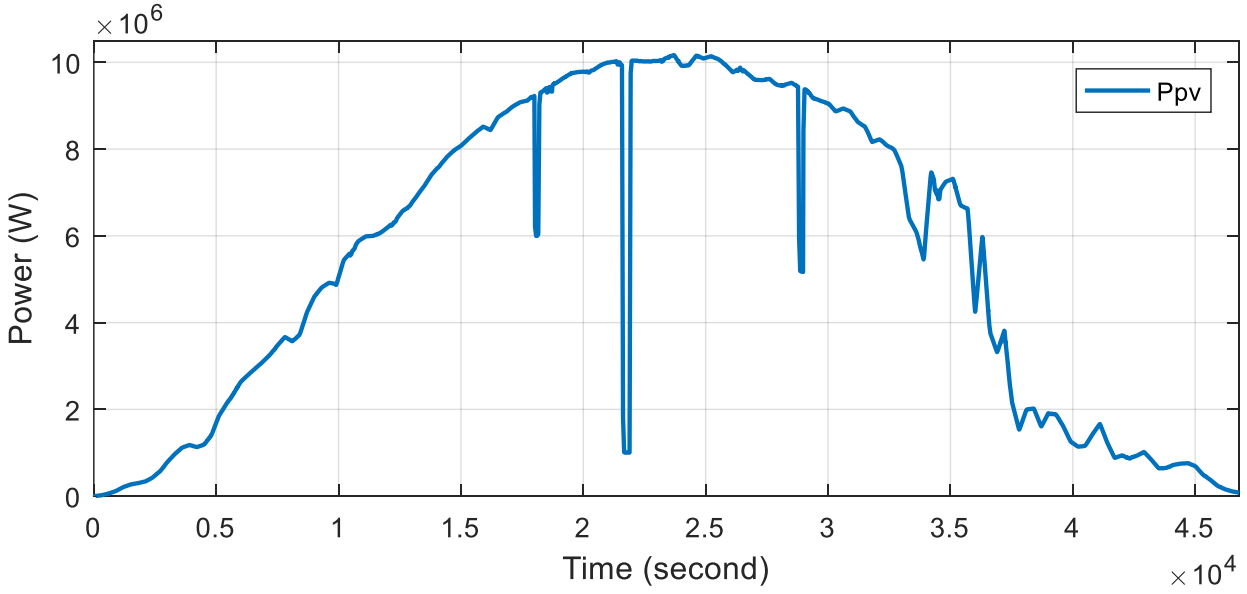

Figure 4-3: PV Power Profile.

With the load profile presented before and the PV active power, the resulting voltage behave is presented in figure 4-4. The results show a tolerance to the first partial shade, but not for the second one with 90% drop of PV production. It is easy to see in the first shade how voltage touch the boundaries. The second shade cold represent the worst case scenario with the maximum PV generation and a power drop of 90% making the voltage at PCC unstable.

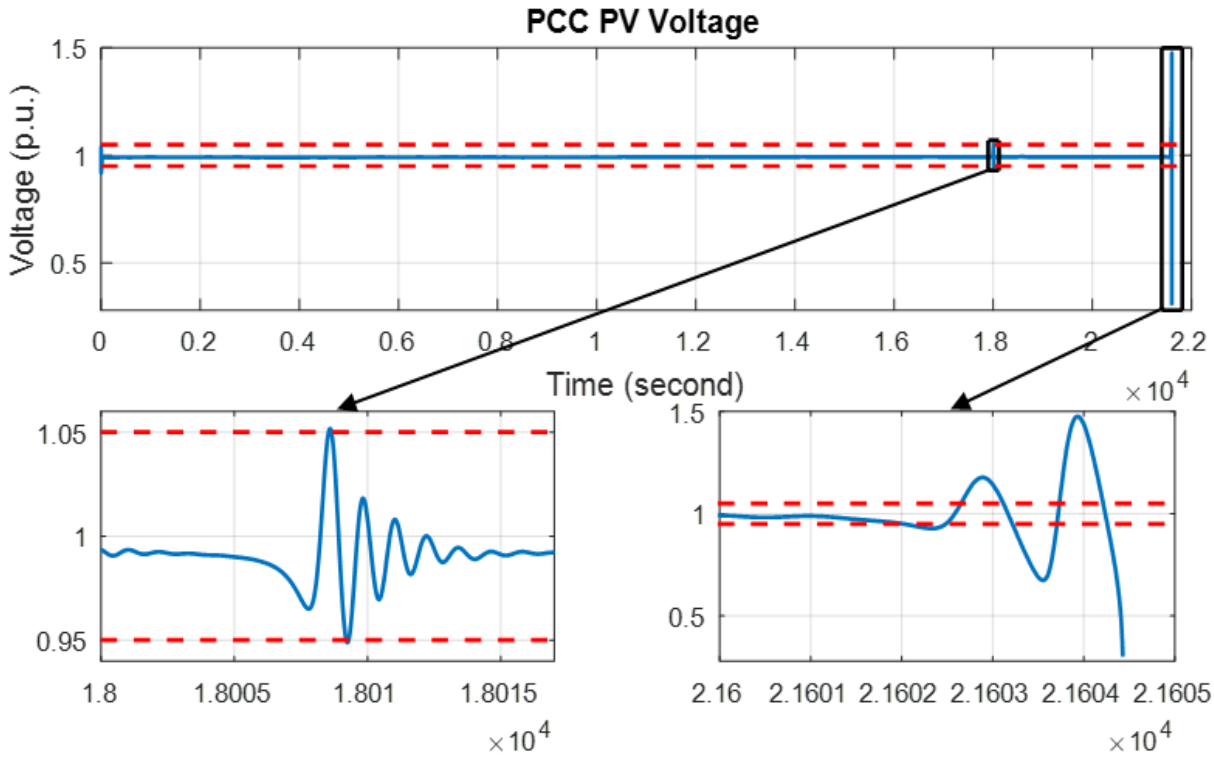

Figure 4-4: Voltage at PCC without Control Strategy.

4.1.3 Third Case

This case introduces STATCOM control acting against the negative effect of PV integration over line voltage. STATCOM control was set for voltage regulation and intentionally used without any energy storage model. The idea is to see how STATCOM deal with voltage regulation without the restriction of the energy storage model could bring on it. Maximum output power was limited to 8.6 MVA as was calculated with equation 3-8. Figure 4-5 present the result of the reactive power provided from STACOM. As show this figure, three notable perturbation are created by the effect of the PV integration. Each perturbation is related with each partial shade discussed in the previews case. It's clear to see that in the last two partial shades, how reactive power reach the boundaries of the maximum power allowed by the energy storage.

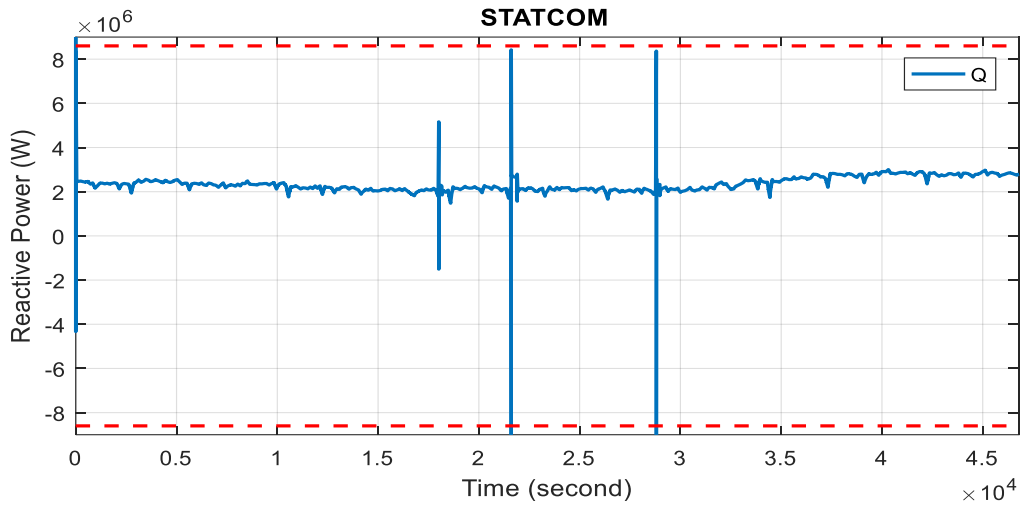

Figure 4-5: STATCOM Reactive Power.

Figure 4-6 shows the corresponding voltage respond to this case. As we can see at the first partial shade, STATCOM control deal very well with the voltage regulation, but with the other two partial shades seems that STATCOM can't. The system uses it maximum capacity of reactive power and it is not enough to keep the voltage within the boundaries. Also, we note that the voltage violates the limits only when the ramp down event occur. As could be expected, with higher droop percentage in PV power, higher and longer is the amplitude of the disturbance over the time.

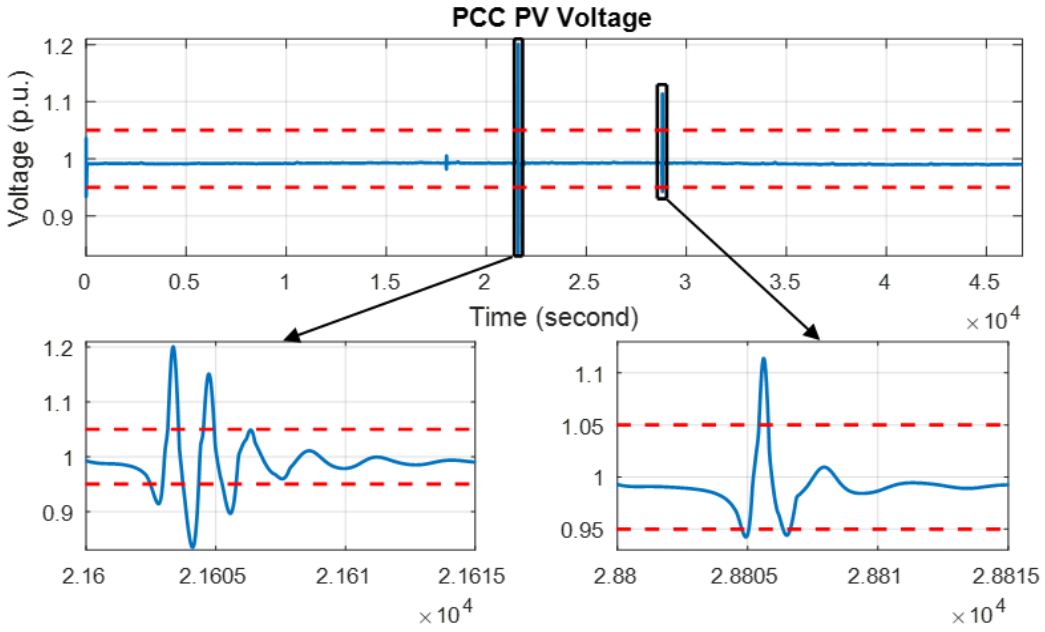

Figure 4-6: Voltage at PCC with STATCOM.

To evaluate if ramps of PV power are under limits, we take samples of PV power every 60 seconds and then, calculate the difference between segment. To obtain the percentage, the result is divided between the rated power of PV farm. Ramp rate percentage is calculated with the following equation:

$$\%rr(t) = \frac{|P_{PV}(t) - P_{PV}(t - \Delta t)|}{P^*} * 100 \quad (4\text{-}1)$$

The minimum technical requirement stipulated by PREPA says, the maximum percentage of ramp rate allowed at the PCC is 10%/min. Figure 4-7 present the ramp rate related with the changes in power from the PV farm. Results shows that a system with only STATCOM control, is not enough to satisfy the minimum requirement when extreme events occurs with the power fluctuations.

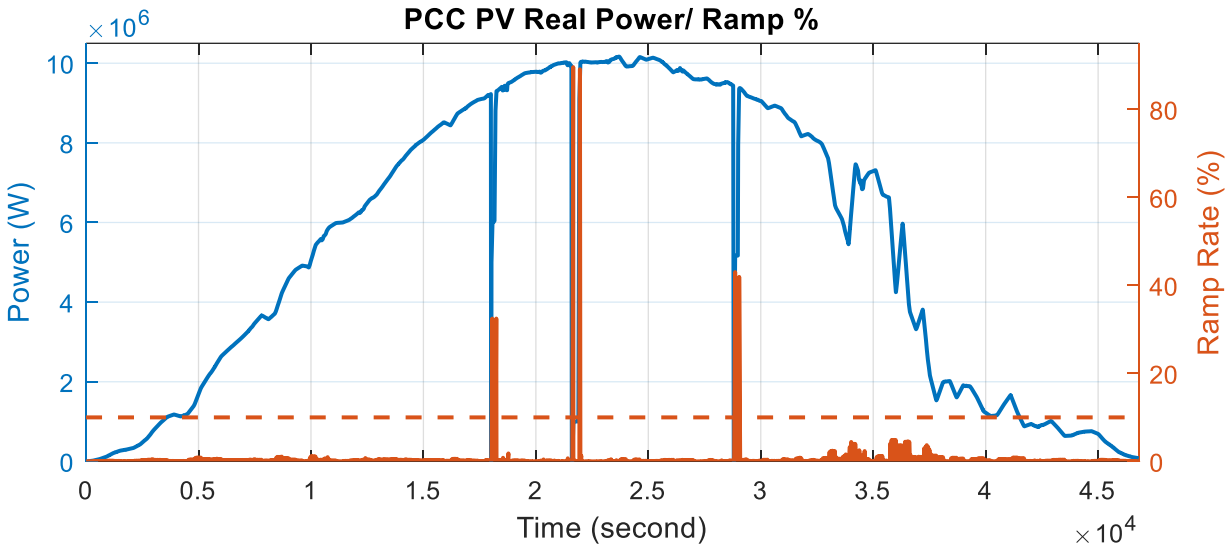

Figure 4-7: PV Power/ Ramp Rate (STATCOM).

4.1.4 Forth Case

Now, this case introduces just the ramp rate control strategy against PV fluctuations that we present with equation 3-4. Also, we introduce the flywheel model proposed in the previous section. We test our model using the same load profile, the generator and the PV integration that we used in the previews cases. As a result, Figure 4-8 shows a comparison of the PV vs what we

call before as $P_G(t)$ in equation 3-4 which is the equivalent to $P_{PV} + P_{fw}$. In other words, P_G is the smoothing PV power by the flywheel through absorbing or released power at the PCC.

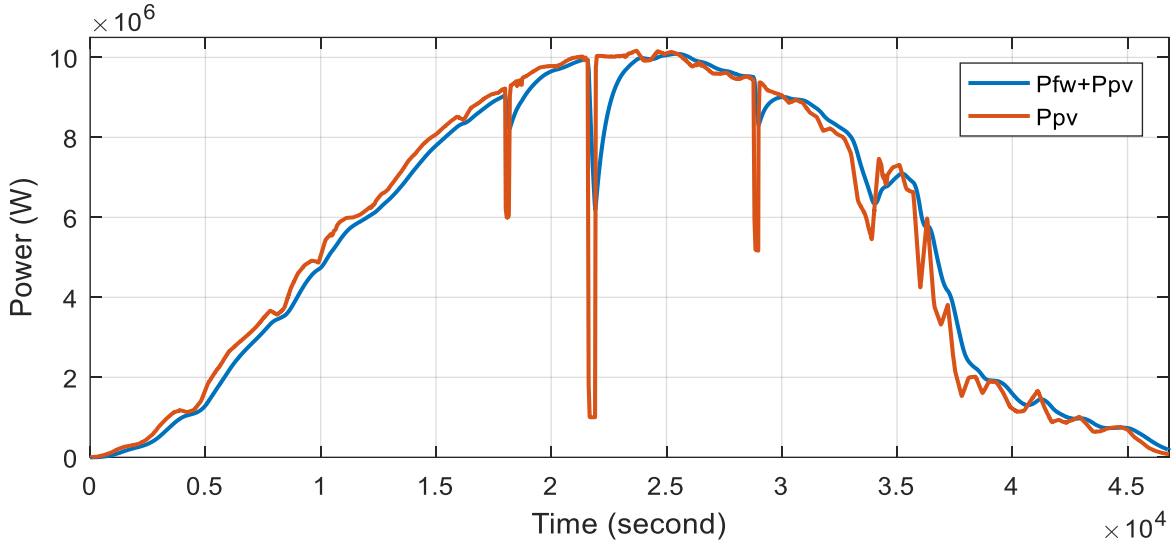

Figure 4-8: PV Power / P_G.

We configure our flywheel model to absorb power when it is negative and supply when it is positive which means that, flywheel is charging or discharging when the power is negative or positive respectively. Without any SOC control, we decide intentionally to set the initial SOC at 20%. The flywheel response to this case is presented in figure 4-9. In this figure, we can see the power absorbed or released by the flywheel and it state of charge behave during the time. Also, can be validated our previous calculation in what it is our worst case scenario at 90% power droop of PV power. Flywheel power reach it maximum power capacity at the 90% ramp down. Figure 4-10 presents the corresponding ramp (up/down) percentage per minute at PCC to see if ramp control complies with ramp rate limit. The ramp control used deal effectively keeping under limit the ramp rate percentage and validate our calculations in the previews section.

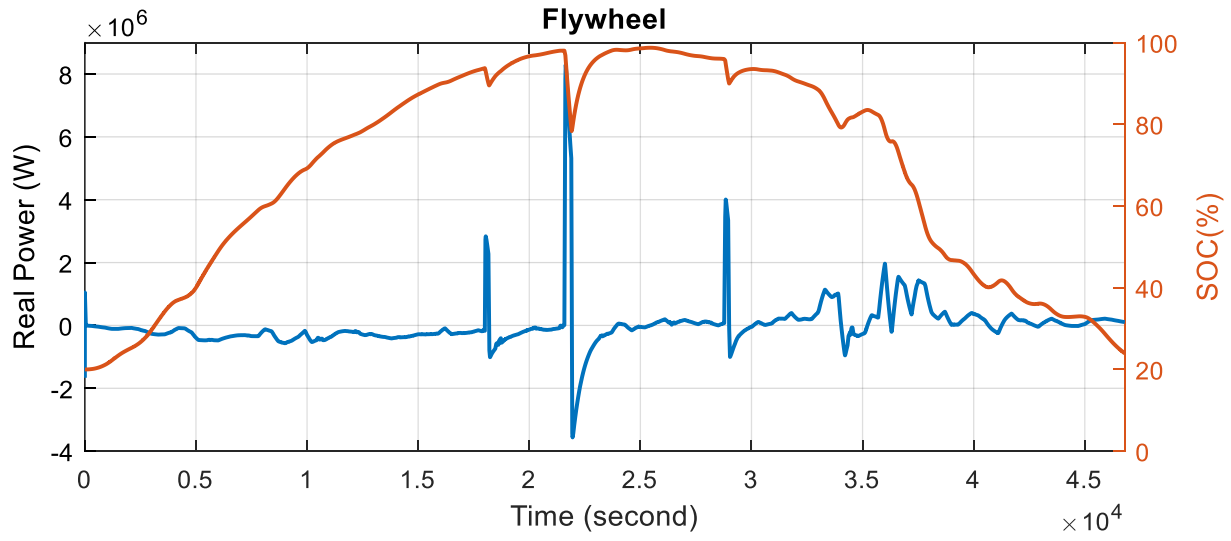

Figure 4-9: Flywheel Power / SOC.

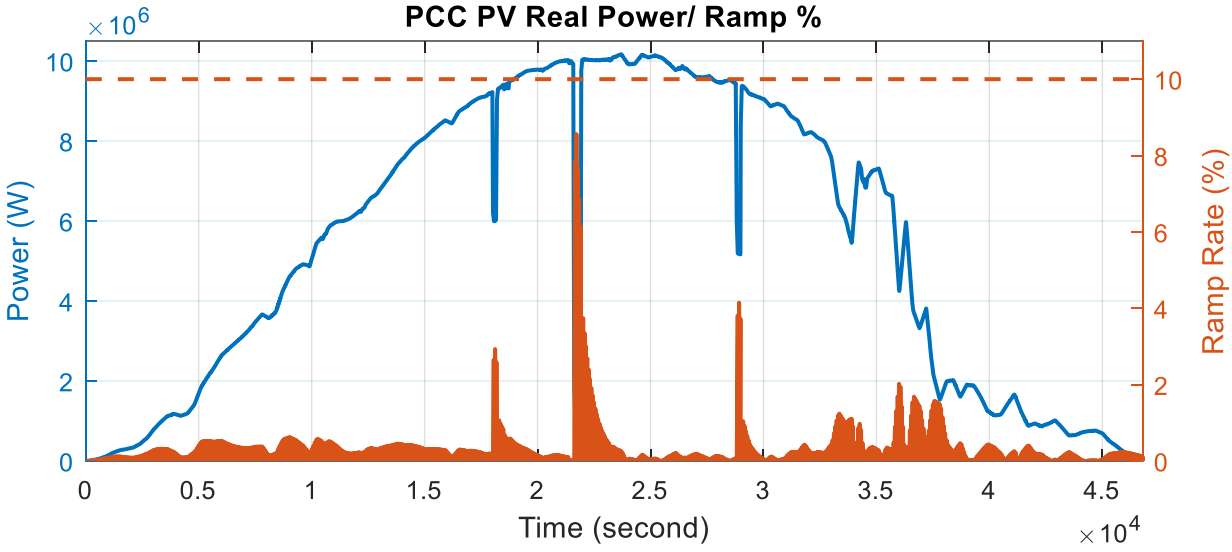

Figure 4-10: PV Power/ Ramp Rate (Ramp Control).

Finally, figure 4-11 present the resulting voltage at PCC. Results indicate that by smoothing power of PV integration at PCC, the voltage can be keep under parameters. We can't say that ramp control is a voltage regulator because it is not a control designed to act with voltage stability, but, it is evident how this can help to avoid voltage instability.

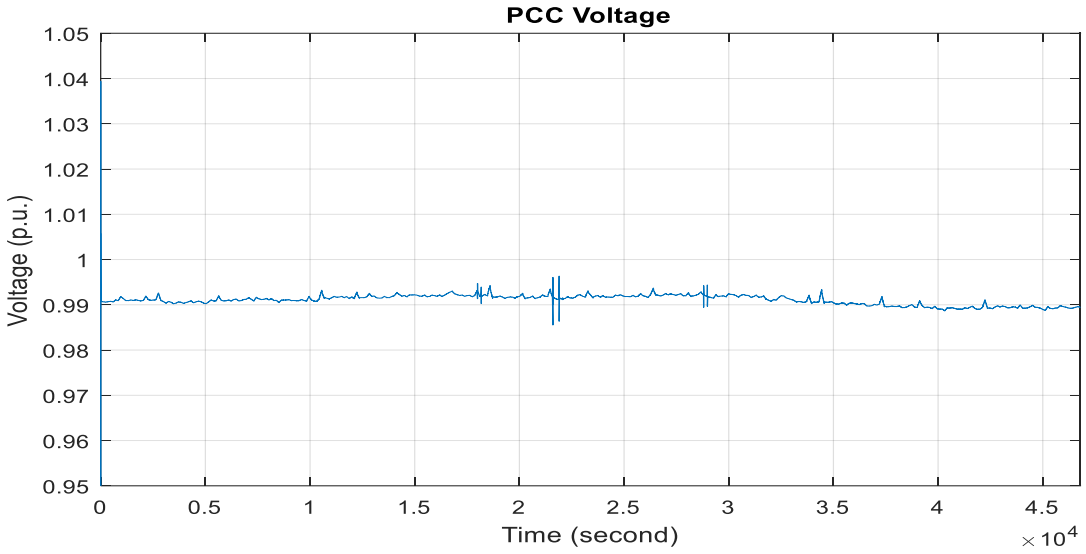

Figure 4-11: Voltage at PCC with Ramp Control.

4.1.5 Fifth Case

This final case intends to compare the performance of flywheels and batteries using STATCOM and ramp rate control to increase PV penetration into the grid and maintain voltage stability. As in the previous case, initial SOC was set at 20%. Both energy storage technologies were evaluated under same circumstances. Results are showing up next.

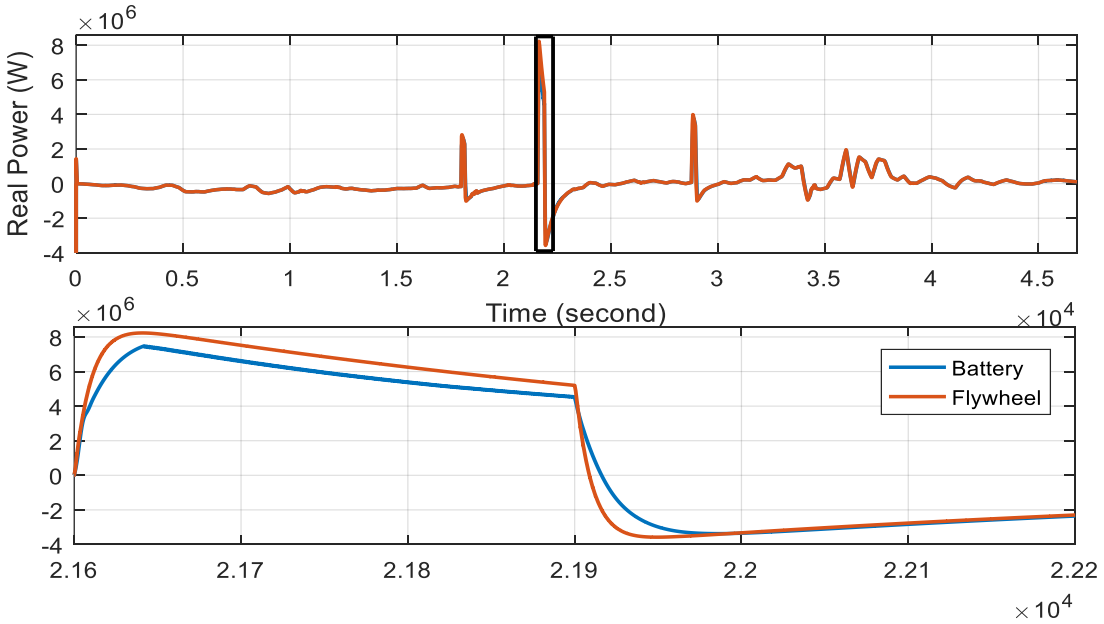

Figure 4-12: Active Power of Flywheel/Battery.

The previews figure shows the performance of both energy storage technologies remarking its qualities to absorb and supplies real power. The bottom image on figure 4-12 is a closer look on the square marker of the upper image. The same marker at the same time are presented in figure 4-13 and 4-14 for the reactive and apparent power respectively showing us the performance of both technologies. We can see when both technologies are pushed to their limit power capacities, it is when we can appreciate their own characteristic. Due to flywheel characteristic of charge and discharge at same rate and it fast capacity to deliver power, flywheel stand out over this kind of battery technology. This lack speed response of the battery forced STATCOM control to work harder as we can see in figure 4-13. The noise presented in the reactive signal of battery maybe cold be mitigated by tuning the control gains but, as we said before, our intention is to compare both energy storage under every same condition.

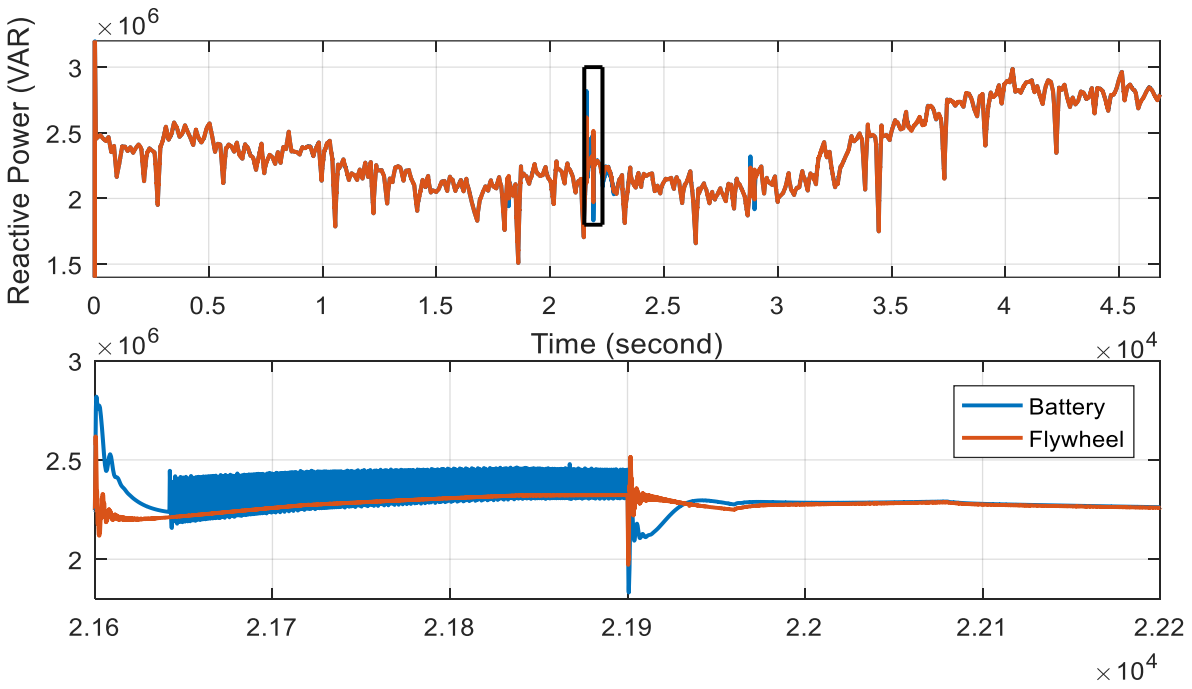

Figure 4-13: Reactive Power of Flywheel/Battery.

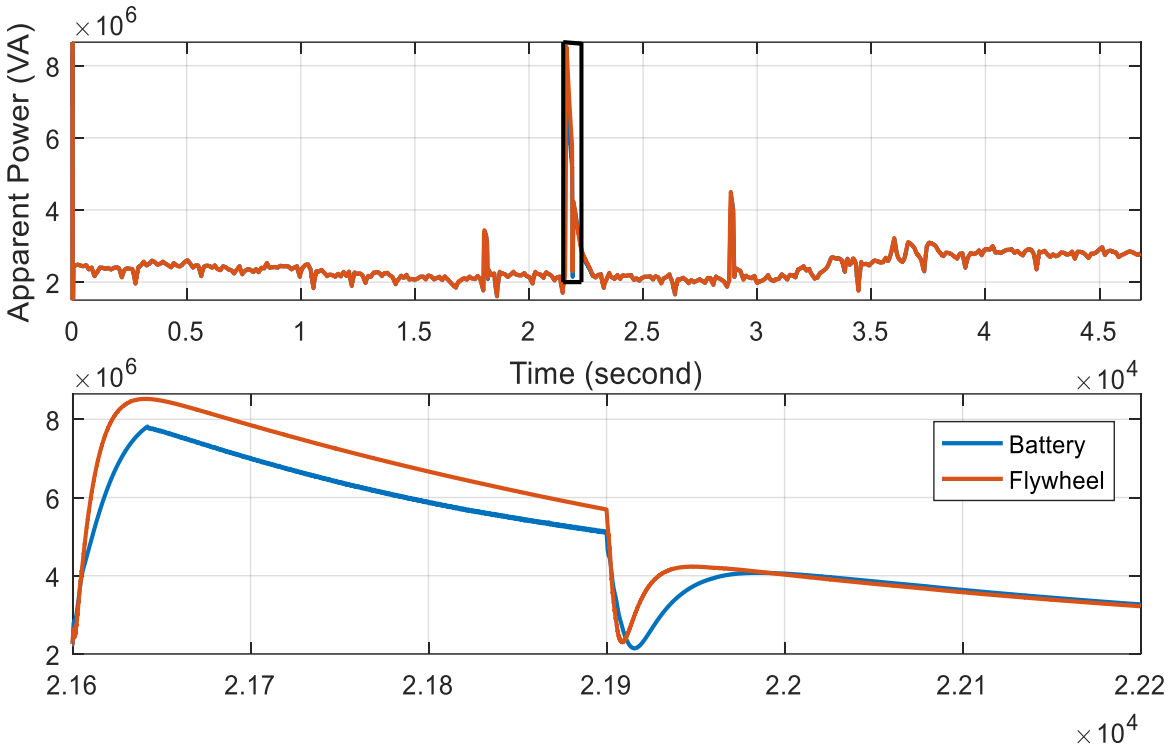

Figure 4-14: Apparent Power of Flywheel/Battery.

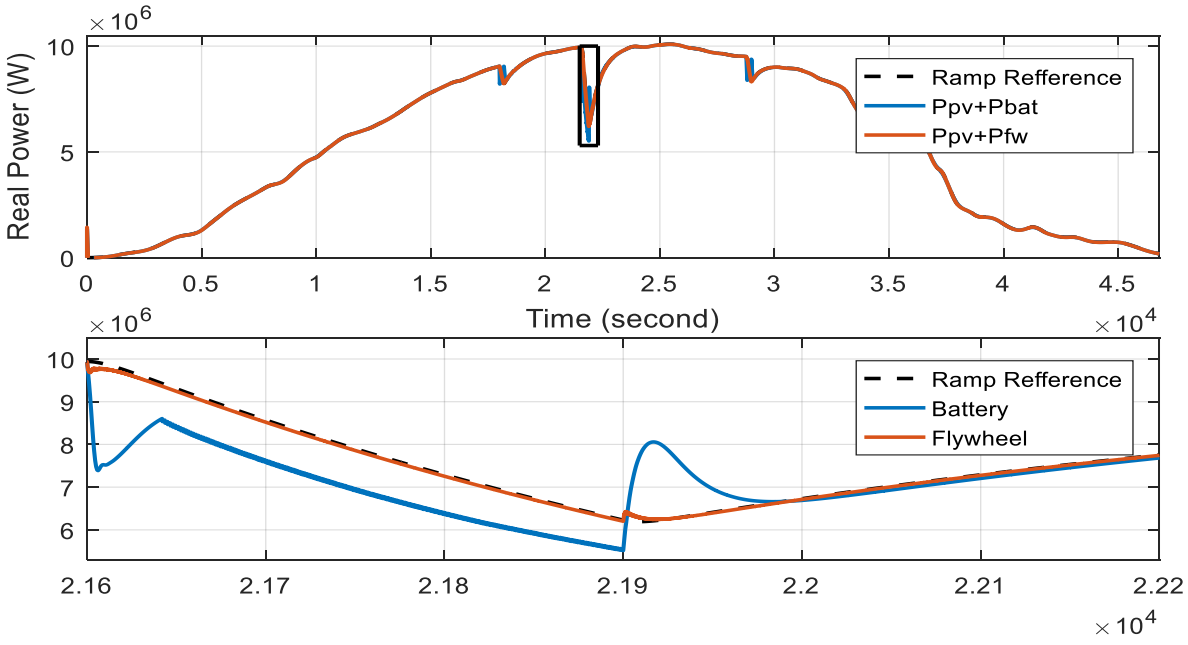

Figure 4-15: P_G Flywheel/Battery.

Figure 4-15 present the resulting power injected into the grid from the PV farm plus the energy storage at PCC. The black dashed line is the power smoothing reference calculated during the simulation from the measured PV power. We can see how the resulting P_G with the help of the flywheel almost overlap the reference signal. The effect of both technologies over the ramping up/down power is presented in figure 4-16. As a result, flywheel keep the ramp rate percentage under 10% limit reaching almost 9% unlike battery which reach around 17%.

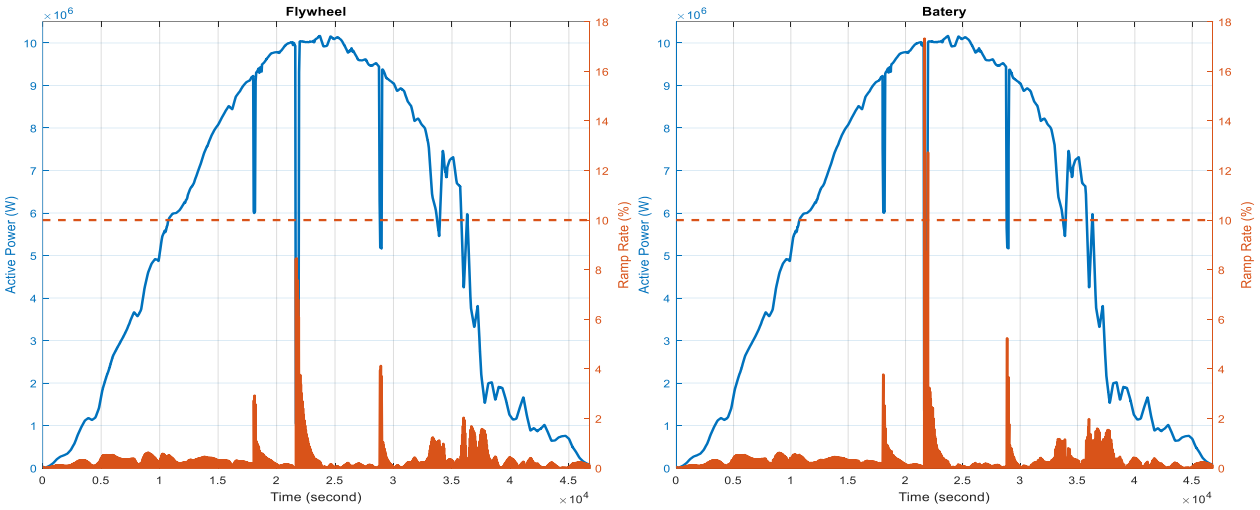

Figure 4-16: PV Power/ Ramp Rate.

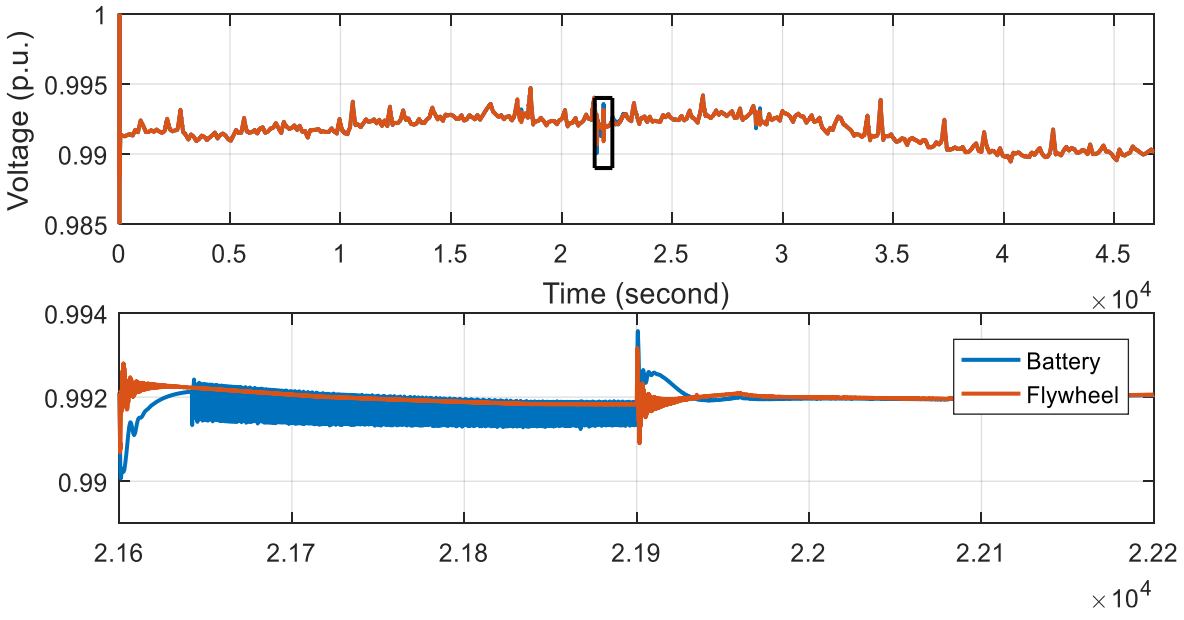

Figure 4-17: Voltage at PCC Flywheel/Battery.

Both technologies could keep voltage under control during the worst events. But, when give a closer look, the one with batteries, tends to be noisier, which it is something that could affect the harmonics level on the signal. Figure 4-18, present the SOC of both technologies starting at 20%. The limitation of batteries to charge at the same rate of discharge it is notable on this figure. Finally, figure 4-19 present the performance of apparent power by each component of this study.

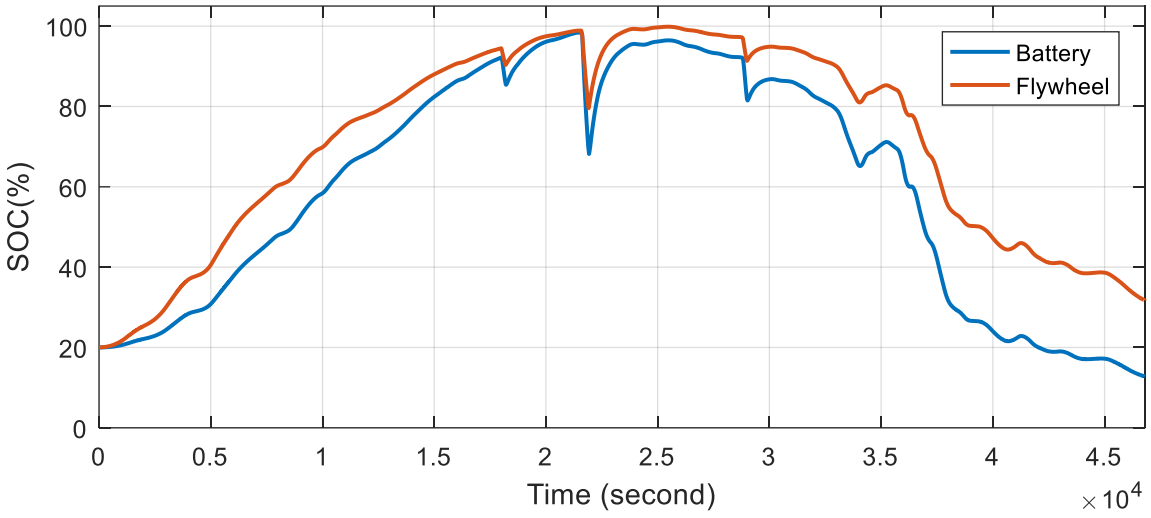

Figure 4-18: SOC Flywheel/Battery.

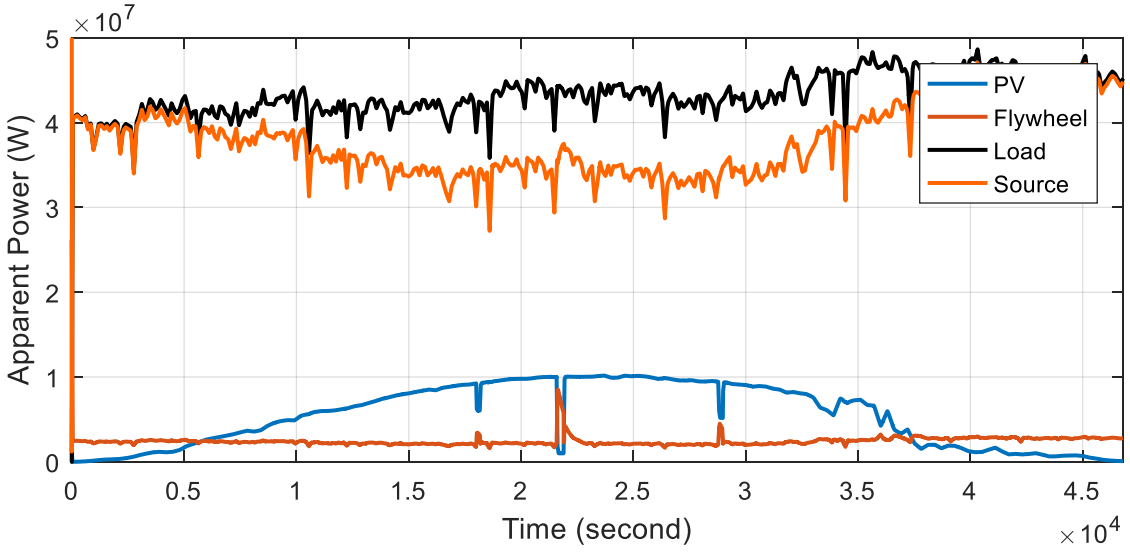

Figure 4-19: Apparent Power by Sources.

4.2. Discussion

We see how flywheels and batteries prove to be effectively to smooth the PV power and avoid voltage instability. Due to it fast response to absorb/supply power and charge and discharge at the same rate, flywheel it is more capable to keep the ramp rate per minute under limits. Also, the use reactive power at it maximum capacity previously calculate is not enough to regulate the voltage at PCC. Although, STATCOM control it is aim for voltage regulation, our results demonstrate that a power smooth technique is more effectively to avoid voltage instability.

Equations in the methodology for power and energy storage required are based on an ideal case. Due to the capabilities of the different energy storage, it is necessary to fit the power capacities base on it minimum. For example, batteries at low level of SOC could not absorb/supply power at the same levels than higher SOC. Due to variation of the output voltage of the battery, is difficult to estimate this quantity of power since manufacturers only provides characteristic of ampere-hour rates.

Chapter 5 - Conclusion and Future Work

5.1. Conclusion

The purpose of this work was to compare battery and flywheels specifically to smooth power and avoid the negative effect over grid voltage caused by PV power rapid fluctuations. To this end, a simulation was conducted considering a conventional generator model as a main source, a proposed variable load profile, a PV source and an energy storage models (based on manufacturer specs) with a ramp rate and STATCOM control. The battery and flywheel model were evaluated under the same circumstances and almost same energy and power capacities.

From result we can conclude a few things bases on our objectives. First, high penetration levels of PV generation could collapse the power electric system turning it in a total blackout. Furthermore, an energy storage sizes needs to be calculated based on a predicted or real data (at least in minutes samples) considering the possible worst case scenario and the allowable ramp rate percentage required by the power authority. The energy storage capacity of both confirm that power smooth technique relies more into power capacity than storage since this application is not for long term storage. Although STATCOM it is aim for voltage regulation, results demonstrate that reactive power is not enough to fight PV fluctuation meanwhile ramp control presented a better performance avoiding voltage instability even though it is not aim for voltage regulation. Shot-term energy storage has demonstrated to help the integration of high percentage of PV energy and keep the system stability within limits. Finally, can be concluded that flywheel as an element to smooth PV power fluctuation and mitigate its secondary effects, it has better response than this specific kind of batteries. We must keep in mind the existence of plenty of batteries that could be a better contender for flywheels.

5.2. Future Work

This work has presented a valuable information to give basis to future works. Today, most of economic analysis are based on 1 hour time series data. Since energy storage technologies relies on discharge cycles to define they lifetime period, it is necessary to have at least a 1 minute time series data or less to conduct a good economic analysis. Due to existence of plenty type of batteries, it is more difficult to realize a performance evaluation between each one because it is necessary to have a reliable dynamic model for any kind. This work shows that power capacity of the energy storage it is more important than energy capacity. Which means, if a battery can't supply power at the same rate required, you must adjust your numbers of batteries. These statements make's not to obvious a decision form initial cost of the energy storage bank since the initial cost per energy capacity of the flywheel its higher than batteries. This is something that could change everything in your economic analysis. Also, wind speed data could be integrated on this kind of study to estimate the displacement velocity of clouds which is the main reason of the rapid variations of PV power generation. A comparison of long and short term energy storage should be developed complying with the minimum technical requirements for a feasibility economic analysis. This analysis could help PREPA to increase percentages of renewable energy making this market more attractive to private investors.

In term of control, could be considered a close loop strategy related with SOC of the energy storage to decide if absorb or supply power depending of SOC percentage. A design a ramp control to use the energy storage only when ramp rate percentage is near to N value could help to reduce the size of ESS including a forecasting technique. Long term energy storage could be combined to schedule the use of conventional generators to make more reliable the energy from PV

generation. Also, the PV power could be curtailed and store the extra power to keep a constant injection into the power gird and analyze the effect on the power quality and economic analysis.

References

[1] Energy Information Administration, "Act 82 of 2010, Public Policy on Energy Diversification by Means of Sustainable and Alternative Renewable Energy in Puerto Rico Act.," 2010. [Online]. Available: http://www.oslpr.org/download/en/2010/A-0082-2010.pdf. [Accessed: 05-Aug-2016].

[2] AEE, "Distribución Porcentual de la Generación de Energía por Tipo Años Fiscales." [Online]. Available: http://www.aeepr.com/Documentos/Ley57/Ley 57 Fuentes de Generación (Portal).pdf. [Accessed: 05-Aug-2016].

[3] SIEMENS, "PREPA Renewable Generation Integration Study," 2014.

[4] J. Marcos, L. Marroyo, E. Lorenzo, D. Alvira, and E. Izco, "Power output fluctuations in large scale pv plants: One year observations with one second resolution and a derived analytic model," *Prog. Photovoltaics Res. Appl.*, vol. 19, no. 2, pp. 218–227, 2011.

[5] J. Marcos, O. Storkël, L. Marroyo, M. Garcia, and E. Lorenzo, "Storage requirements for PV power ramp-rate control," *Sol. Energy*, vol. 99, pp. 28–35, Jan. 2014.

[6] S. Shivashankar, S. Mekhilef, H. Mokhlis, and M. Karimi, "Mitigating methods of power fluctuation of photovoltaic (PV) sources - A review," *Renew. Sustain. Energy Rev.*, vol. 59, pp. 1170–1184, 2016.

[7] K. M. Farahani, "Modeling and analysis of a flywheel energy storage system for voltage regulation," Ryerson University, Canada, 2012.

[8] R. van Haaren, M. Morjaria, and V. Fthenakis, "An energy storage algorithm for ramp rate control of utility scale PV (photovoltaics) plants," *Energy*, vol. 91, pp. 894–902, 2015.

[9] R. A. Presentation, "Consulting engineers annual report on the electric property of the puerto rico power authority," Cambridge, MA, 2013.

[10] "Contratos Compra de Energia Renovable y Enmiendas." [Online]. Available: http://www.aeepr.com/Docs/TablasProyRenovablesAgosto232013.pdf. [Accessed: 09-May-2015].

[11] V. Gevorgian and S. Booth, "Review of PREPA technical requirements for interconnecting wind and solar generation," Golden, CO, 2013.

[12] CRE, "Reglas generales de interconexion al sistema electrico nacional." [Online]. Available: http://econotecnia.com/descargas/Comprimido/REGLAS INTERCONEXION SEN.compressed.pdf. [Accessed: 05-Jan-2018].

[13] Eskom Transmission Division, "Grid connection code for renewable power plants connected to the electricity transmission system or the distrubution system in South Africa," vol. 2.8, no. July, p. 17, 2014.

[14] G. Arias, "Modelado y simulacion de dispositivos fotovoltaicos," University of Puerto Rico Mayaguez Campus, 2009.

[15] E. I. Ortiz-rivera, S. Member, F. Z. Peng, and I. Fellow, "Analytical Model for a Photovoltaic Module using the Electrical Characteristics provided by the Manufacturer Data Sheet," *2005 IEEE 36th Conf. Power Electron. Spec.*, no. June 12, 2005, pp. 2087–2091.

[16] M. G. Molina, *Dynamic modelling and control design of advanced energy storage for power system applications*, no. January. Croatia: INTECH, 2010.

[17] B. Bolund, H. Bernhoff, and M. Leijon, "Flywheel energy and power storage systems," *Renew. Sustain. Energy Rev.*, vol. 11, pp. 235–258, 2007.

[18] G. R. Barai, "Optimization of Hybrid Energy Storage System Providing Power Curve Smoothening in Grid Scale," Ryerson University, Canada, 2016.

[19] M. Dürr, A. Cruden, S. Gair, and J. R. McDonald, "Dynamic model of a lead acid battery for use in a domestic fuel cell system," *J. Power Sources*, vol. 161, no. 2, pp. 1400–1411, 2006.

[20] D. Francisco, "Contributions of flywheel systems in wind power plants," Universitat Politecnica de Catalunya, 2013.

[21] IEC, "Electrical energy storage - White paper," *Int. Electrotech. Comm.*, pp. 1–78, 2011.

[22] "US Department of Energy: Global energy storage database." [Online]. Available: http://link.springer.com/10.1007/s40565-015-0134-y. [Accessed: 26-Jan-2018].

[23] G. L. Kyriakopoulos and G. Arabatzis, "Electrical energy storage systems in electricity generation: Energy policies, innovative technologies, and regulatory regimes," *Renew. Sustain. Energy Rev.*, vol. 56, pp. 1044–1067, 2016.

[24] D. Rastler, "Electricity energy storage technology options: A white paper primer on applications, costs, and benefits," EPRI, Palo Alto, CA, 2010.

[25] A. A. Akhil *et al.*, "DOE/EPRI Electricity storage handbook in collaboration with NRECA," Albuquerque, NM, 2015.

[26] S. Swaminathan and R. K. Sen, "Review of power quality applications of energy storage systems," Sandia National laboratories, Albuquerque, New Mexico, Report., 1998.

[27] R. Gustavsson, S. Hussain, and A. Saleem, “Ancillary services for smart grids - Power quality markets,” *2013 IEEE Grenoble Conf. PowerTech, POWERTECH 2013*, 2013.

[28] E. Hirst and B. Kirbv, “Electric-power ancillary services,” Oak Ridge, Tennesse, 1996.

[29] J. San Martin, I. Zamora, V. Aperriba, and P. Eguia, “Energy storage technologies for electric applications,” International Conference on Renewable Energies and Power Quality, Spain, 2011.

[30] E. A. J. Brea, E. I. Ortiz-rivera, A. Salazar-llinas, and J. Gonzalez-llorente, “Simple photovoltaic solar cell dynamic sliding mode controlled maximum power point tracker for battery charging applications,” Palm Springs, California, 2010.

[31] SolarWorld, “SW 275 MONO BLACK,” SW275 datasheet,2014.

[32] “Beacon Power-Flywheel Energy Storage System-Technology Overview.” [Online]. Available: http://beaconpower.com/wp-content/themes/beaconpower/inc/beacon_power_brochure_081414.pdf. [Accessed: 15-May-2017].

[33] M. Garcia-Plaza, D. Serrano-Jimenez, J. Eloy-Garcia Carrasco, and J. Alonso-Martinez, “A Ni-Cd battery model considering state of charge and hysteresis effects,” *J. Power Sources*, vol. 275, pp. 595–604, 2015.

[34] SAFT, “SPH Ni-Cd battery Instant power,”SPH 11 datasheet, April. 2007.

[35] J. Marcos, I. de La Parra, M. García, and L. Marroyo, “Control strategies to smooth short-term power fluctuations in large photovoltaic plants using battery storage systems,” *Energies*, vol. 7, no. 10, pp. 6593–6619, 2014.

[36] I. de la Parra, J. Marcos, M. García, and L. Marroyo, “Storage requirements for PV power ramp-rate control in a PV fleet,” *Sol. Energy*, vol. 118, pp. 426–440, 2015.